

**Descriptive text to the Geological map  
of Greenland, 1:100 000, Kangaatsiaq  
68 V.1 Syd and Ikamiut 68 V.1 Nord**

Adam A. Garde and Julie A. Hollis

## Geological Survey of Denmark and Greenland Map Series 5

### Keywords

Geological mapping, Archaean, Nagssugtoqidian orogen, Palaeoproterozoic ocean floor, crustal reworking, zircon geochronology

### Cover

Extract of the western part of the Kangaatsiaq map sheet showing Archaean rocks reworked during the Palaeoproterozoic Nagssugtoqidian orogeny. The main components are arc-related metasedimentary and metavolcanic rocks embedded within younger orthogneiss and Kangaatsiaq granite. The prominent NE–SW-trending structural grain is due to Nagssugtoqidian tectonic reworking.

### Frontispiece: facing page

Mesoarchaean synkinematic granite displaying pygmatic folding, emplaced into polyphase orthogneiss in the southern part of the Aasiaat domain that is unaffected by Palaeoproterozoic Nagssugtoqidian tectonic reworking. Island at the head of Saqqarput 34.3 km south-east of Kangaatsiaq.

*Chief editor of this series:* Adam A. Garde

*Scientific editor of this volume:* Ole Bennike

*Editorial secretaries:* Jane Holst and Esben W. Glendal

*Referee:* Sandra Piazzolo (Sweden)

*Illustrator:* Adam A. Garde

*Digital photographic work:* Benny M. Scharck

*Graphic production:* Henrik K. Pedersen

*Printers:* Rosendahls · Schultz Grafisk a/s, Albertslund, Denmark

*Manuscript received:* 3 March 2009

*Final versions approved:* 6 October 2010

*Printed:* 30 December 2010

ISSN 1604-9780

ISBN 978-87-7871-295-0

### Citation of the name of this series

It is recommended that the name of this series is cited in full, viz. Geological Survey of Denmark and Greenland Map Series.

If abbreviation of this volume is necessary, the following form is suggested: Geol. Surv. Den. Green. Map Series 5, 41 pp. + 2 maps.

### Available from

Geological Survey of Denmark and Greenland (GEUS)

Øster Voldgade 10, DK-1350 Copenhagen K, Denmark

Phone: +45 38 14 20 00, fax: +45 38 14 20 50, e-mail: [geus@geus.dk](mailto:geus@geus.dk)

or at [www.geus.dk/publications/maps](http://www.geus.dk/publications/maps)

© De Nationale Geologiske Undersøgelser for Danmark og Grønland (GEUS), 2010

For the full text of the GEUS copyright clause, please refer to [www.geus.dk/publications/maps](http://www.geus.dk/publications/maps)



# Contents

<b>Abstract</b> .....	7
<b>Introduction</b> .....	9
Adjacent map sheets .....	10
Field work .....	10
Physiography .....	11
<b>Aeromagnetic and geochronological data</b> .....	11
Geochronological data .....	12
<b>Geological background and previous interpretations</b> .....	13
Lithological components .....	13
Previous interpretations .....	13
Archaean and Palaeoproterozoic map units and their division .....	14
<b>Archaean map units</b> .....	15
Archaean orthogneiss complex and remobilised granitic rocks .....	15
Orthogneiss, mainly tonalitic ( <b>gn</b> ) .....	15
K- and Si-metasomatised orthogneiss ( <b>gm</b> ) .....	16
Dioritic orthogneiss ( <b>di</b> ) .....	17
Granodioritic orthogneiss ( <b>gr</b> ) .....	17
Granite ( <b>g</b> ) .....	19
Granitic and pegmatitic veins ( <b>p</b> ) .....	20
Archaean supracrustal and related intrusive rocks: main components and relationships with orthogneiss .....	20
Amphibolite ( <b>a</b> ) .....	21
Metagabbro ( <b>ai</b> ) .....	21
Anorthosite and leucogabbro ( <b>an</b> ) .....	23
Ultrabasic rocks ( <b>ub</b> ) .....	23
Biotite schist and paragneiss ± garnet and/or sillimanite ( <b>s</b> ) .....	23
Quartzo-feldspathic paragneiss ( <b>q</b> ) .....	24
Marble and calcareous rocks ( <b>m</b> ) .....	24
<b>Palaeoproterozoic map units</b> .....	25
Naternaq supracrustal belt at Naternaq/Lersletten: main components and structure .....	25
Amphibolite ( <b>na</b> , <b>na</b> <sub>2</sub> ) .....	26
Biotite ± muscovite schist, commonly with garnet, staurolite and/or sillimanite ( <b>ns</b> ) .....	26
Marble and calc-silicate rocks ( <b>c</b> ), and volcanogenic-exhalative horizons with chert and sulphidic rocks ( <b>v</b> ) .....	26
Metavolcanic and metasedimentary rocks on Isuamiut–Qaqqarsuatsiaq and Equutiit Killiat islands and Hunde Ejlande north-east and north of Aasiaat .....	27
Greenstone: pillow lava ( <b>π</b> ) and sill complex ( <b>na</b> <sub>1</sub> , <b>na</b> <sub>3</sub> ); garnet-bearing greenstone ( <b>ng</b> ) .....	29
Staurolite-andalusite-muscovite-biotite-garnet schist ( <b>ss</b> <sub>1</sub> , <b>ss</b> <sub>3</sub> ) .....	29
Chlorite schist ( <b>cs</b> ) with intercalations of sandstone ( <b>mm</b> ), chert ( <b>cq</b> ), banded iron formation and calcareous rocks .....	29
Metadolerite ( <b>m</b> ) .....	30
Granite and pegmatite ( <b>gp</b> , <b>P</b> ) .....	30
<b>Cretaceous–Paleocene rocks</b> .....	31
Basalt, picritic ( <b>b</b> ) .....	31
Sandstone ( <b>st</b> ) .....	31
Dolerite dykes ( <b>δ</b> ) .....	31
<b>Quaternary deposits</b> .....	32
<b>Archaean crustal evolution</b> .....	32
The Aasiaat domain: a distinct Archaean crustal segment .....	32

Archaean crustal accretion in arc environments, and evidence of Archaean rifting and sedimentation at the margins of the proto-Aasiaat domain .....	32
<b>Palaeoproterozoic tectonic evolution and plate-tectonic model</b> .....	33
<b>Economic geology</b> .....	35
<b>Acknowledgements</b> .....	36
<b>References</b> .....	36
<b>Appendix: zircon U-Pb geochronological data</b> .....	39
Sample preparation and analytical methods .....	39
Orthogneiss 467558, island east of Maniitsoq .....	39
K-feldspar porphyritic granodiorite 467565 and 467575, Maniitsoq and adjacent island .....	40



# Abstract

Garde, A.A. & Hollis, J.A. 2010: Descriptive text to the Geological map of Greenland, 1:100 000, Kangaatsiaq 68 V.1 Syd and Ikamiut 68 V.1 Nord.  
*Geological Survey of Denmark and Greenland Map Series 5*, 41 pp. + two maps.

The two adjacent Kangaatsiaq and Ikamiut map sheets cover a coastal area of central West Greenland in the northern part of the Palaeoproterozoic Nagssugtoqidian orogen. The map area is part of the Aasiaat domain, which almost entirely consists of Neoarchaean orthogneisses with intercalated metamorphosed volcano-sedimentary belts. The Aasiaat domain was partially reworked during the Nagssugtoqidian orogeny, but Palaeoproterozoic components are restricted to mafic dykes, the  $\leq 1904 \pm 8$  Ma (2 $\sigma$ ) Naternaq supracrustal belt east of Kangaatsiaq, and remnants of a *c.* 1850 Ma Palaeoproterozoic ocean-floor – arc-trench association on small islands north-east of Aasiaat. Undated, lithologically similar rocks occur on Hunde Ejlande north of Aasiaat.

The Archaean volcano-sedimentary belts are up to 2 km thick and comprise fine-grained mafic and minor, intermediate amphibolite of ex- and intrusive origin, gabbro, leucogabbro-anorthosite, and biotite-garnet schist with common sillimanite pseudomorphs after andalusite. The *c.* 2.8 Ga Archaean orthogneiss is largely tonalitic besides minor dioritic and granodioritic components, and preserves intrusive relationships with some of the supracrustal belts. Sheet-like bodies of late-kinematic crustal melt granites are up to about 10 km in length and 2 km thick. One of these has yielded a zircon Pb-Pb age of  $2748 \pm 19$  Ma (2 $\sigma$ ). Up to kilometre-thick units of quartzo-feldspathic and locally garnet-bearing paragneisses also occur, some of which are younger than the orthogneisses.

The Aasiaat domain has undergone two Archaean orogenic episodes, separated by injection of mafic dykes and sedimentation at its margins. Archaean deformation resulted in kilometre-scale, tight to isoclinal folds refolded by upright to overturned folds, and its southern part reached granulite facies *P–T* conditions with widespread partial melting. The Aasiaat domain also underwent heating during the Nagssugtoqidian orogeny, but only its northern part was tectonically reworked, resulting in an intense E–W- to NNE–SSW-trending structural grain associated with subhorizontal extension lineation.

The Palaeoproterozoic Naternaq supracrustal belt in the eastern part of the Kangaatsiaq map area has a complex synformal structure and displays a prominent structural discordance against the underlying Archaean rocks; the belt also contains a second phase of SE-plunging, overturned folds. The Palaeoproterozoic ocean-floor – arc trench association on islands north-east of Aasiaat comprises pillow lava, manganiferous chlorite schist, chert, banded iron formation, graded aluminous schist, and siliceous sandstone, and points to the existence of a palaeosuture in this area.

A Palaeogene picritic sill complex and a small exposure of sandstone form the *c.* 15 km long island group of Kitsissunnguit / Grønne Ejland in the north-eastern Ikamiut map area. Two contemporaneous, N–S-trending mafic dykes were emplaced into the basement rocks south-west of the islands. One of these was hydraulically chilled and fractured during its emplacement, presumably due to contact with meteoric or sea water. Widespread hydrothermal alteration occurs along faults and joints in the basement rocks in the northern archipelago. The alteration may have been caused by circulation of magmatically heated meteoric or sea water during the development of the Cretaceous–Paleocene basalt province in West Greenland.

No deposits of economic interest have been found in the Archaean rocks within the map area. A massive sulphide deposit in the Naternaq supracrustal belt was discovered and explored in the 1960s by Kryolitselskabet Øresund A/S, and a VHMS-style copper-gold-zinc mineralisation was reported in 2004 from Kitsissuarsuit / Hunde Ejlande by a local inhabitant. The potential for ornamental rocks is largely unexplored.

---

#### Authors' addresses

A.A.G., *Geological Survey of Denmark and Greenland, Øster Voldgade 10, DK-1350 Copenhagen K, Denmark.*

E-mail: [aag@geus.dk](mailto:aag@geus.dk)

J.A.H., *Northern Territory Geological Survey, PO Box 3000, NT 0801, Australia*

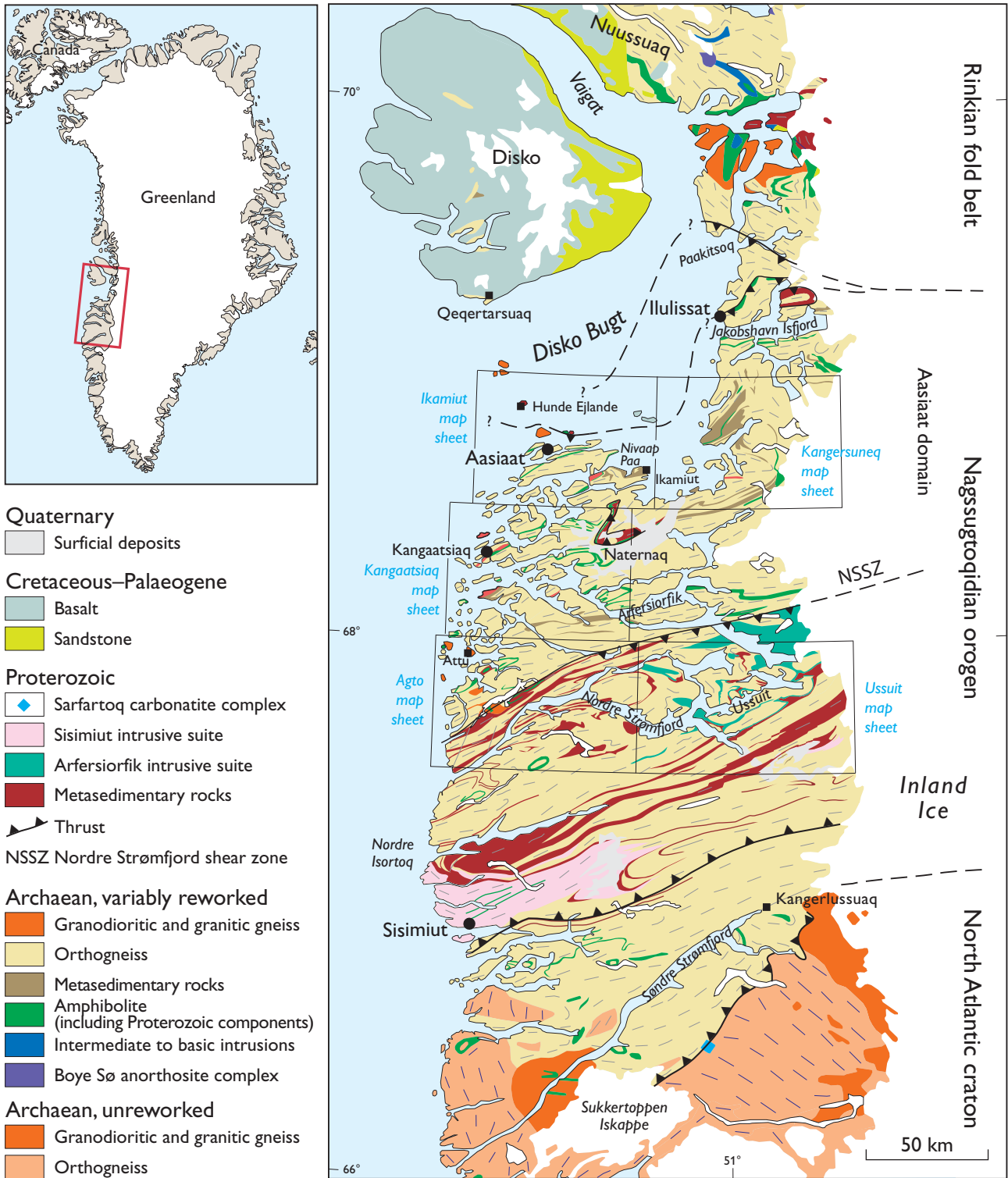


Fig. 1. Geological map of the Nagssugtoqidian orogen in West Greenland with tectonic divisions and the locations of published 1:100 000 geological maps (modified from van Gool & Marker 2007). The northern boundary of the Asiaat domain with its associated Palaeoproterozoic ocean-floor rocks is drawn so that it follows the change of the magnetic signatures in Fig. 4, and is tentatively correlated with the palaeosuture north of Ilulissat proposed by Connelly *et al.* (2006). The southern boundary of the Asiaat domain is located along the previously identified Nordre Strømfjord shear zone (see van Gool *et al.* 2002), where NNW-directed Palaeoproterozoic thrusting occurs e.g. at the head of Ataneq (see Fig. 19); the rocks along the westernmost part of the Nordre Strømfjord shear zone are near-vertical or dip steeply towards SSE.





Fig. 3. View towards the north-east over the southern part of Naternaq/Lersletten. A meandering river system flows through the Quaternary outwash plain of raised silty, white-grey, shallow marine deposits. A low ridge in the distance exposes Precambrian bedrock.

islands north-east of Aasiaat and at Naternaq/Lersletten. A few Palaeogene olivine-phyric basaltic dykes occur in the northern and eastern parts of the map area; the contemporaneous island group of Kitsissunnguit / Grønne Eiland in the north-east exposes picritic basalt and a small outcrop of sandstone.

### Adjacent map sheets

Three 1:100 000 scale map sheets in the vicinity of the Kangaatsiaq and Ikamiut sheets have previously been published. The Agto map sheet 67 V.1 N (Olesen 1984) directly south of the Kangaatsiaq map sheet that straddles the boundary between the Aasiaat domain and the central Nagssugtoqidian orogen and was mapped in the 1960s and 1970s. The map units were mainly defined and mapped according to their mineral parageneses, mostly without distinction between igneous and sedimentary protoliths. This approach displayed the distribution of metamorphic facies very clearly, but impeded correlation with the subsequently published Kangaatsiaq and Ussuit map sheets, where the map units are largely based on recognition of protoliths (van Gool & Marker 2007).

The Ussuit map sheet 67 V.2 N itself (van Gool & Marker 2004) south-east of the Kangaatsiaq map area was based on work by the Danish Lithosphere Centre (1994–1999) and a final field season with two teams in 2000. There is no direct geological overlap with the present work. The Ussuit map sheet is located south of the Aasiaat domain, in the eastern part of the central Nagssugtoqidian orogen and comprises Palaeoproterozoic supracrustal rocks, the contemporaneous Arfersior-

fik intrusive complex, and in its southern part intensely reworked Archaean rocks belonging to the North Atlantic craton.

The Kangersuneq map sheet 68 V.2 S (van Gool 2005) east of the Ikamiut map sheet was produced almost concurrently with the latter sheet, hence there are no breaks in the map units in the contact area south-east of Ikamiut (Fig. 1). This map sheet in the north-eastern part of the Aasiaat domain almost exclusively consists of variably reworked Archaean rocks; no Palaeoproterozoic supracrustal rocks have been discovered. The Archaean orthogneisses and supracrustal belts in the boundary area between the two map sheets are cut by sporadic, deformed Palaeoproterozoic mafic dykes, which document Palaeoproterozoic tectonic overprinting in this area.

### Field work

The first geological study in the northern Nagssugtoqidian orogen by the Geological Survey of Greenland (GGU) took place already in 1948, when Ellitsgaard-Rasmussen (1954) mapped and described the well-preserved metavolcanic and metasedimentary rocks occurring on some small islands north-east of Aasiaat (see later sections). Later, Noe-Nygaard & Ramberg (1961) and Henderson (1969) carried out coastal reconnaissance investigations for GGU, which included the northern Nagssugtoqidian orogen. The latter investigation was undertaken for the 1:500 000 scale geological map sheet Søndre Strømfjord – Nûgssuaq (Escher 1971). The region was visited again in the 1990s by the Danish Lithosphere Centre, when Kalsbeek & Nutman (1996) and Whitehouse *et al.* (1998) carried out reconnaissance geochronological studies.

Henderson's (1969) work and his unpublished coastal maps in the Survey archives served as a convenient starting point for the subsequent systematic mapping of the Kangaatsiaq, Ikamiut and Kangersuneq map areas undertaken in 2001–2003 by the Geological Survey of Denmark and Greenland (GEUS) and an international group of geologists. Based on this work three geological maps on a scale of 1:100 000 were published by Garde (2004, 2006) and van Gool (2005). Most of the field work for the Kangaatsiaq and Ikamiut map sheets described here was performed using rubber dinghies along the coasts and supplemented by a few foot traverses and limited helicopter-supported work in inland areas. Index maps on the two map sheets display the positions of all 2001–2003 ground observation points as recorded by satellite positioning along with the names of the mapping geologists. The field work was supplemented by interpretation of black and white aerial photographs on a scale of 1:150 000 by the first author, but apart from accurate

delineation of faults and areas covered by surficial Quaternary deposits only limited geological information could be extracted in this way.

### Physiography

Much of the Kangaatsiaq–Ikamiut map area forms an archipelago that is easily accessible by boat (Fig. 2). The mainland is relatively flat with elevations up to 450 m, dissected by several ENE- and ESE-trending fjords. Exposure is excellent in the intertidal zone and reasonable on south-facing slopes, whereas north-facing slopes

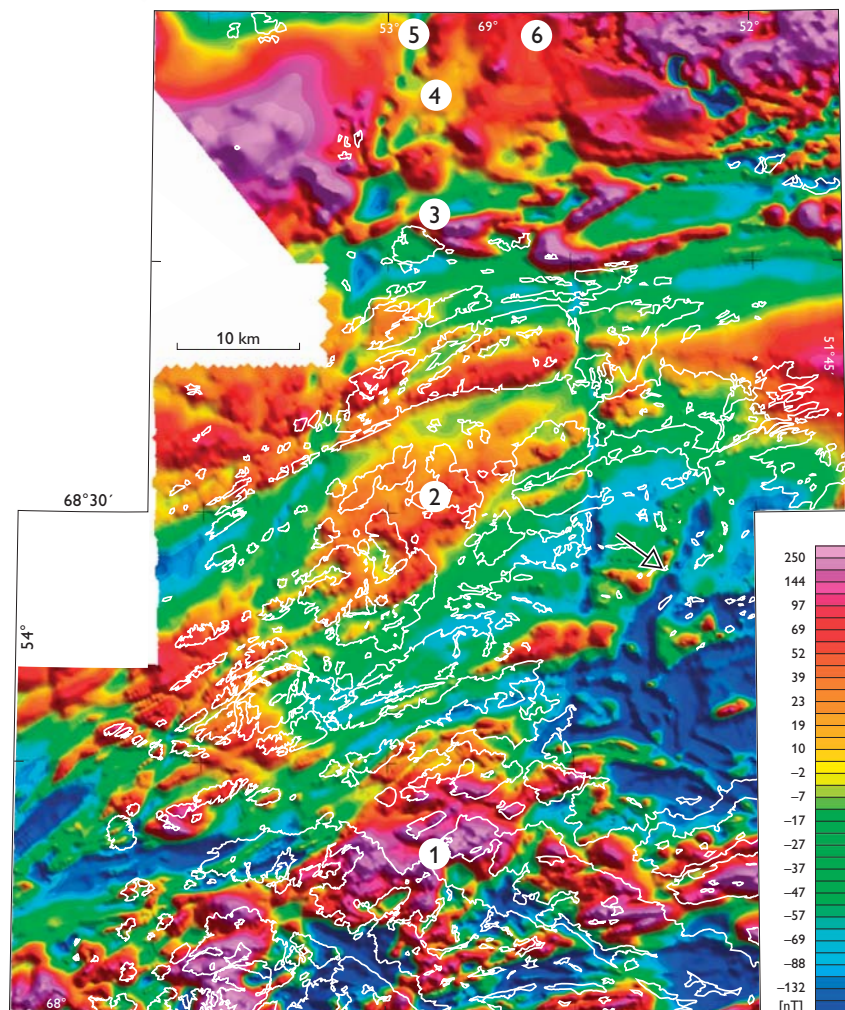
in inland areas are commonly overgrown by lichens or thick blankets of moss. The map area also comprises the protected Naternaq/Lersletten wetland area, a periglacial outwash plain of raised shallow marine deposits which is an important area for breeding and moulting of greater white-fronted geese (Fig. 3). The sediment was derived from the glacier Akuliarutsip Sermersua / Nordenskiöld Gletscher east of the Kangaatsiaq map area. The scattered rounded hills of exposed bedrock within the Naternaq area are somewhat difficult to access except by helicopter.

## Aeromagnetic and geochronological data

Most of the map area is covered by high-quality aeromagnetic maps (Thorning 1993; Rasmussen & van Gool 2000). Nielsen & Rasmussen (2004) produced interpretative aeromagnetic maps from the northern Nagssugto-

qidian orogen from this data set. Maps of the total magnetic intensity (Fig. 4A) and the vertical gradient of the latter (Fig. 4B) clearly delineate several important features, labelled 1–6 and with an arrow. The southern part

Fig. 4A. Aeromagnetic map of the northern Nagssugtoqidian orogen showing total magnetic intensity. (1) tectonically unreworked southern Aasiaat domain with open, curved magnetic signatures. (2) central and northern Aasiaat domain with strong ENE-trending linear pattern due to intense Nagssugtoqidian reworking. Arrow at Naternaq supracrustal belt with low total intensity and angular discordance between its N–S-trending western flank and ENE-trending basement structures. (3) ENE-trending belt of narrow high and low magnetic intensity zones at the northern plate boundary of the Aasiaat domain outlining a simple fold pair. (4) smooth signature of high magnetic intensity, likely underlain by homogeneous granitic rocks of Archaean age. (5, 6) Palaeogene dolerite dykes, trending almost N–S. See main text for references and discussion.



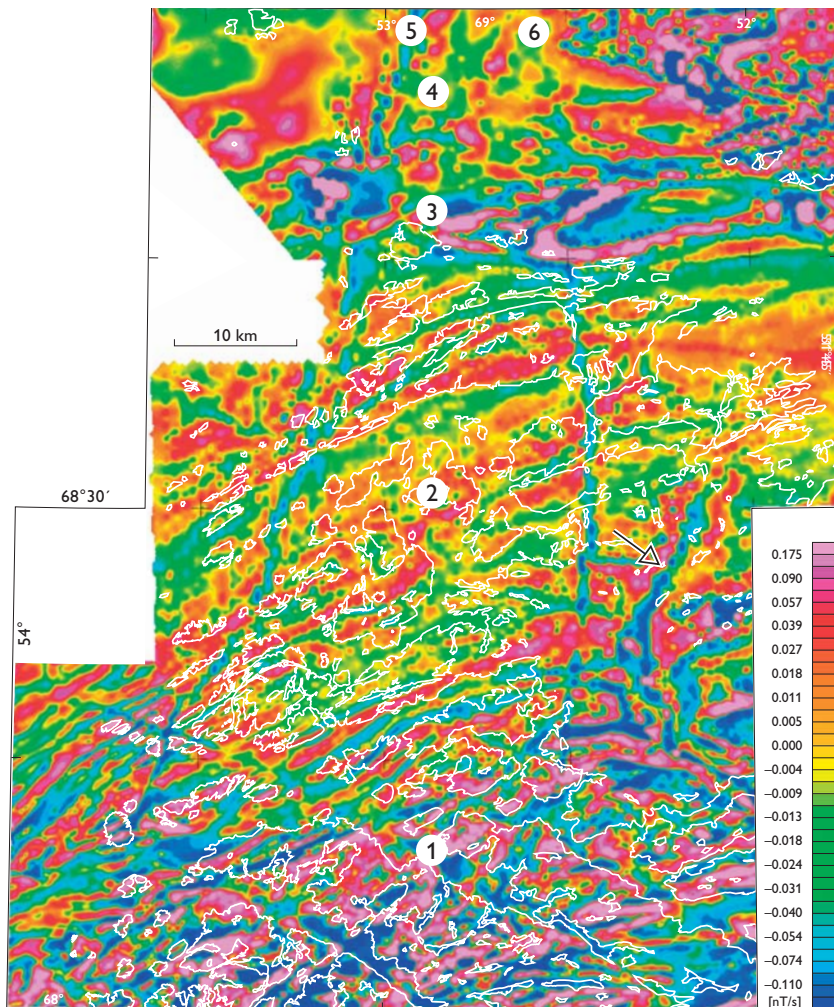


Fig. 4B. Aeromagnetic map of the northern Nagssugtoqidian orogen: vertical gradient of the total magnetic intensity. (1) tectonically unreworked southern Aasiaat domain with open, curved magnetic signatures. (2) central and northern Aasiaat domain with strong ENE-trending linear pattern due to intense Nagssugtoqidian reworking. Arrow at Naternaq supracrustal belt with low total intensity and angular discordance between its N–S-trending western flank and ENE-trending basement structures. (3) ENE-trending belt of narrow high and low magnetic intensity zones at the northern plate boundary of the Aasiaat domain outlining a simple fold pair. (4) smooth signature of high magnetic intensity, likely underlain by homogeneous granitic rocks of Archaean age. (5, 6) Palaeogene dolerite dykes, trending almost N–S.

of the map area (1) displays open, curved magnetic signatures and corresponds to the tectonically unreworked part of the Archaean Aasiaat domain (described later). The central part of the map area (2) displays a strong ENE-trending linear pattern due to intense Nagssugtoqidian reworking of the northern Aasiaat domain. In this area there is also a marked magnetic low (viz. a strong vertical gradient) in the area of the Naternaq supracrustal belt, and a major angular discordance is visible between ENE-trending basement structures and the N–S-trending western flank of the Naternaq supracrustal belt. This discordance is addressed in later sections.

The southernmost part of Disko Bugt, north of Aasiaat, displays a very distinct, ENE-trending belt about 10 km wide (3). This belt is characterised by narrow zones with alternating high and low magnetic intensities, which outline a pair of prominent fold-like structures. The southern margin of the belt warps around Maniitsoq island and then follows the Isuamiut–Qaqqarsuatsiaq – Equutiit Killiat islands eastwards. Its northern margin straddles Hunde Ejlande (see place names on Fig. 2). This 10 km wide belt with its large, simple, apparent fold structures is interpreted as representing the northern plate boundary of the Aasiaat domain with associated

Palaeoproterozoic rocks along its northern margin. The simple structures indicating open to tight folds resemble the folds that are actually exposed on the Isuamiut–Qaqqarsuatsiaq – Equutiit Killiat islands in the southern part of the belt (see later). The area in Disko Bugt to the north and north-west of the 10 km wide belt has a smooth signature of high magnetic intensity (4). It may be underlain by homogeneous granitic rocks similar to those exposed on nearby Kronprinsen Ejland, which are presumed to be of Archaean age.

Two almost N–S-trending, slightly convergent lines (5 and 6) with low total magnetic intensity and strong vertical gradients dissect the central part of the map area. They correspond to Palaeogene dolerite dykes.

### Geochronological data

This work contains a couple of new ion microprobe U–Pb zircon age determinations of Archaean rocks that are addressed where appropriate in the main text and described in detail in the Appendix. All age data quoted in this publication are given with  $2\sigma$  errors.

# Geological background and previous interpretations

## Lithological components

As mentioned above the Kangaatsiaq–Ikamiut map area is underlain by the Aasiaat domain, most of which consists of Neoproterozoic orthogneiss with interspersed supracrustal belts of generally undated Archaean amphibolite, mica schist ( $\pm$  sillimanite, garnet), and garnet-bearing quartzo-feldspathic paragneiss (Hollis *et al.* 2006; Moyen & Watt 2006; Garde *et al.* 2007a; St-Onge *et al.* 2009; Garde & Hollis 2010). Palaeoproterozoic metavolcanic and metasedimentary rocks are restricted to the Naternaq supracrustal belt in the eastern part of the Kangaatsiaq map area, the islands of Isuamiut–Qaqqarsuatsiaq and Equutiit Killiat about 10 km north-east of Aasiaat, and presumably also the island group of Hunde Ejlande (Garde & Hollis 2010). Metamorphosed mafic dykes of presumed Palaeoproterozoic age have been observed in the archipelago west and north-east of Aasiaat, where they are intensely deformed, and in the southern part of the Aasiaat domain close to 68°N, where they are undeformed. Small bodies of heterogeneous S-type granite occur in the hinge zones of Palaeoproterozoic folds within the Naternaq supracrustal belt, and straight, late-orogenic Palaeoproterozoic pegmatites up to a few metres wide can be found throughout the Aasiaat domain. Rare Palaeogene olivine-phenocrystic mafic dykes occur e.g. in the north-western part of the Ikamiut map area, and a N–S-trending, hydraulically chilled and fractured Palaeogene dyke occurs in its eastern part.

## Previous interpretations

Ramberg (1949) identified the southern boundary of the Nagssugtoqidian orogen by means of the deformation front that affects the Kangâmiut mafic dyke swarm in the Kangerlussuaq / Søndre Strømfjord area between 66 and 67°N. However, the northern limit of the orogen was never firmly established, and the part north of 68°N has not been studied in detail prior to the mapping project in 2001–2003. In the days prior to the recognition of plate tectonics and when also geochronological data were not easily available, the Nagssugtoqidian orogeny was described in terms of *in situ* reworking of Archaean crust, “most likely at the beginning of the Proterozoic or end of the Archaean” (i.e. at around 2.5 Ga, Escher *et al.* 1976; Korstgaard 1979). However, Kalsbeek *et al.* (1978) showed that the Kangâmiut dyke swarm and hence the Nagssugtoqidian orogeny is much younger. Kalsbeek *et*

*al.* (1984) subsequently demonstrated that the central Nagssugtoqidian orogen also comprises at least one juvenile magmatic arc of Palaeoproterozoic age as well as Palaeoproterozoic supracrustal rocks. Kalsbeek *et al.* (1987) furthermore suggested that a cryptic Palaeoproterozoic suture occurs in the central part of the orogen. Studies in 1994–1999 by the Danish Lithosphere Cen-

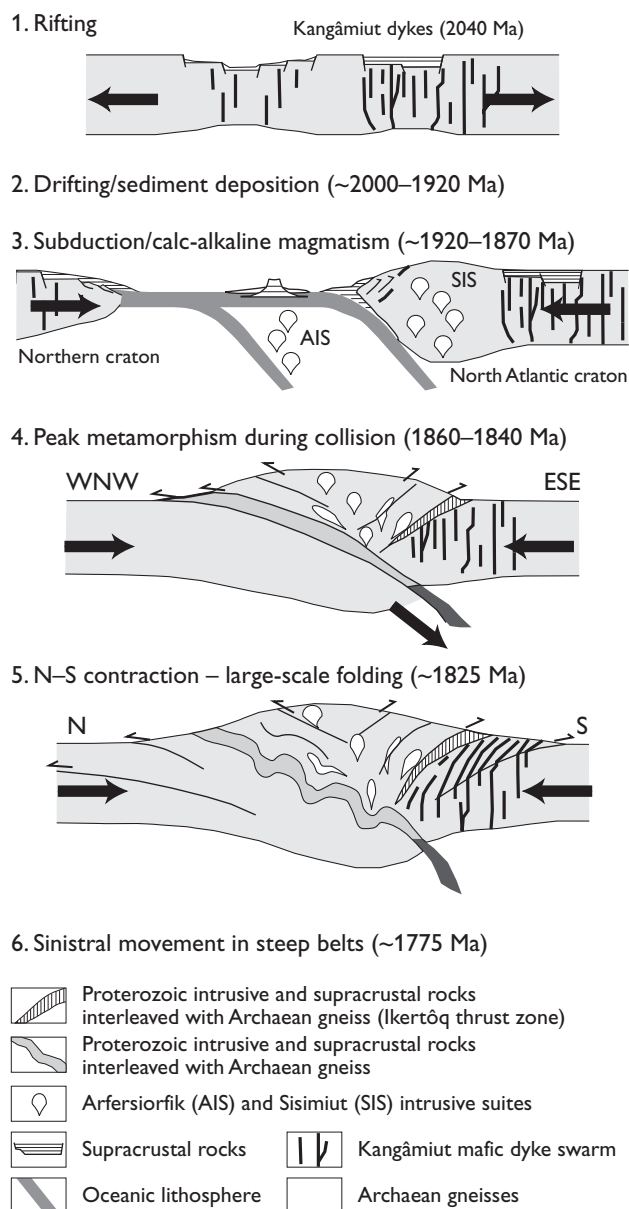


Fig. 5. Plate-tectonic model of the Nagssugtoqidian orogen, slightly simplified from van Gool *et al.* (2002). The now outdated model shows two colliding continents and a single main suture.

tre (DLC) concentrated in the Ussuit area (Fig. 1) led to a collisional plate-tectonic model for the Nagssugtoqidian orogen with a tentative interpretation of southward subduction of a northern collisional plate under the North Atlantic craton, which forms the southern foreland of the orogen (Connelly *et al.* 2000; van Gool *et al.* 2002; van Gool & Marker 2007). The northern plate was not investigated in much detail by the DLC and was thought to be contiguous with the Archaean basement of the Rinkian fold belt farther north. Figure 5 shows a slightly simplified version of this plate-tectonic model; for a general description of the Rinkian fold belt see Henderson & Pulvertaft (1987). The most recent mapping project in the northern Nagssugtoqidian orogen firmly established that the Archaean rocks south and south-east of Kangaatsiaq escaped Palaeoproterozoic deformation (Piazolo *et al.* 2004; Mazur *et al.* 2006; van Gool & Piazolo 2006), and the model of Fig. 5 is now considered outdated (see below, later sections and Garde & Hollis 2010 for further discussion).

Studies in 2001–2003 within the Rinkian fold belt also verified that the Rinkian fold belt is collisional in nature and that the Nagssugtoqidian orogen and the Rinkian fold belt are contemporaneous (Garde *et al.* 2003; Thrane *et al.* 2003; Sidgren *et al.* 2006). Connelly *et al.* (2006) proposed a second south-dipping suture at Paakitsoq (Fig. 1), where a major system of flat-lying, ultramylonitic shear zones is exposed. Garde & Hollis (2010) have subsequently shown that the outcrops of volcanic and sedimentary rocks on the Isuamiut–Qaqqarsuatsiaq and Equutiit Killiat islands north-east of Aasiaat represent Palaeoproterozoic ocean floor and a buried

spreading ridge (see below). According to Garde & Hollis (2010) these rocks have been preserved in a south-dipping palaeosuture at the boundary between the Aasiaat domain and the Archaean Rae craton which underlies the Rinkian fold belt. This model is discussed in a later section.

### **Archaean and Palaeoproterozoic map units and their division**

The Kangaatsiaq and Ikamiut map sheets mostly comprise similar rock units that are contiguous with each other. They are treated together in the following descriptions. The current division between Archaean and Palaeoproterozoic supracrustal rocks is based on a combination of field relationships and age determinations. However, the limited available geochronological data and their uneven geographical distribution imply that some supracrustal rock units mapped as Archaean may in fact be Palaeoproterozoic in age. This is especially the case in areas of intense deformation where primary contact relationships have been completely destroyed, and in the area immediately south of Naternaq where the few existing field observations were made before it was realised that the supracrustal belts comprise both Archaean and Palaeoproterozoic rocks. The supracrustal rocks on Hunde Ejlande north of Aasiaat are shown as Palaeoproterozoic because they are lithologically similar to Palaeoproterozoic rocks north-east of Aasiaat, but geochronological work on Hunde Ejlande is needed to confirm this.

# Archaean map units

## Archaean orthogneiss complex and remobilised granitic rocks

The Archaean orthogneiss complex comprises two main rock associations. The first and most voluminous one comprises polyphase tonalitic–trondhjemitic–granodioritic (TTG) orthogneisses (including minor dioritic rocks). These are commonly migmatised and generally at least moderately deformed, also where Nagssugtoqidian tectonic overprinting is absent. The second association comprises variably porphyritic granites and pegmatites. These are younger and usually less deformed than the TTG orthogneisses and preserve field and compositional evidence of having been derived from orthogneiss precursors by partial melting.

### Orthogneiss, mainly tonalitic (gn)

Medium-grained, biotite- and locally hornblende-bearing, tonalitic to granodioritic orthogneiss is by far the most voluminous rock association in the map area. Such rocks from Ikamiut have been described in some detail by Hollis *et al.* (2006), who also published age data (see below). The metamorphic grade is upper amphibolite facies throughout the central and northern Aasiaat domain; the biotite in the orthogneiss mostly occurs as evenly distributed flakes 2–3 mm long, suggesting that the rocks have not been through granulite facies metamorphism and subsequent retrogression. In the northern archipelago the orthogneiss is commonly homogeneous and porphyritic, with subhedral plagioclase crystals up to 1.5 cm long. Elsewhere the orthogneiss is commonly migmatised with indistinct veinlets of local partial melt origin (Fig. 6A). At the latitudes between Aasiaat and Kangaatsiaq the orthogneiss has obtained an intense, steep, NNE–SSW-trending schistosity and a subhorizontal extensional linear fabric (Fig. 6B–C). The overprinting diminishes southwards and is absent in the southern half of the Kangaatsiaq map area. It is interpreted as a result of the Nagssugtoqidian orogeny (Mazur *et al.* 2006; Thrane & Connelly 2006; Garde & Hollis 2010). The different resulting tectonic styles in the unworked and reworked parts of the Aasiaat domain are clearly visible on the aeromagnetic maps of Fig. 4.

Disrupted relicts of mafic dykes, commonly only a few centimetres thick and in many places folded, have been observed e.g. at Arfersiorfik and Saqqarput in the south-east of the map area (Fig. 7), where Nagssugtoqidian tectonic overprinting is absent. The folded dyke fragments

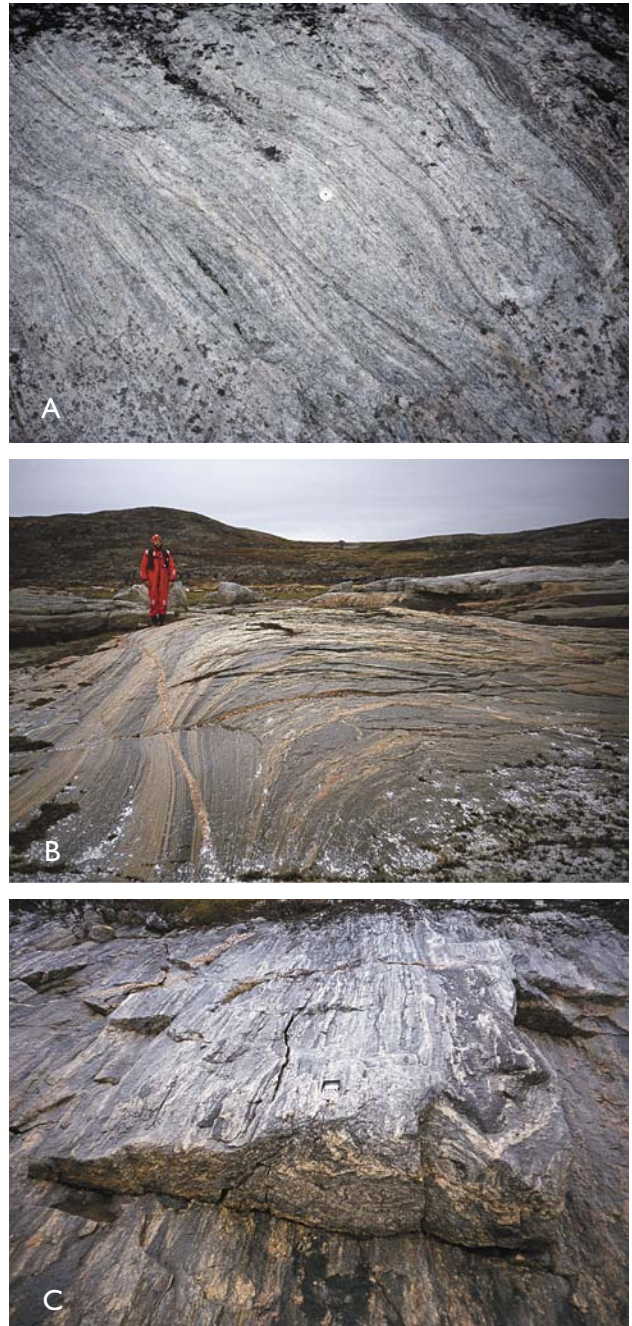


Fig. 6. Orthogneiss in the central and northern Aasiaat domain. A: Deformed polyphase tonalitic orthogneiss with migmatitic partial melt seams just west of the Naternaq supracrustal belt. Coin for scale ( $d = 2.8$  cm). B, C: Archaean orthogneiss with intense Nagssugtoqidian tectonic overprinting, producing intense schistosity on the island of Naajat (B; person for scale) and ENE-trending extension lineation and refolding at embayment east of Naajat (C; compass for scale). Locations shown in Fig. 2.

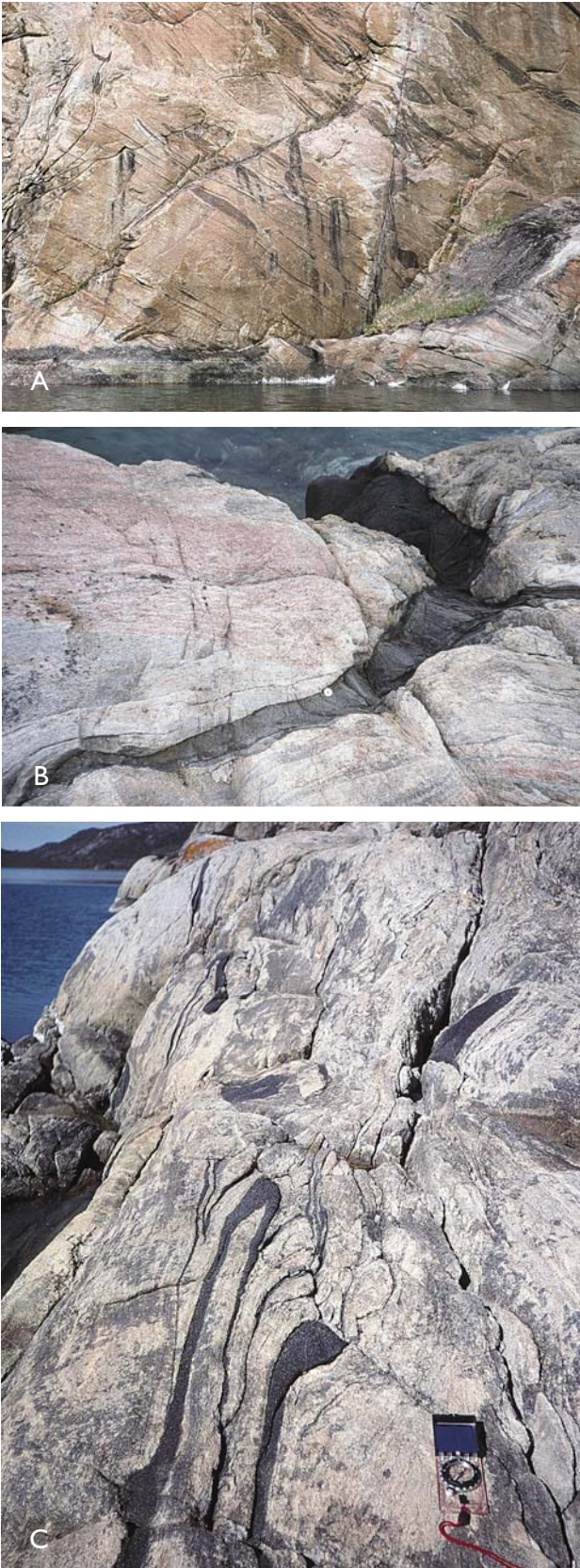


Fig. 7. Archaean orthogneiss in the southern Aasiaat domain with deformed fragments of mafic dykes of presumed Archaean age. **A:** Head of Saqqarput; cliff face about 10 m high. **B:** Southern Saqqarput; coin for scale ( $d = 2.8$  cm). **C:** Northern branch of Arfersiorfik at eastern boundary of map area, with compass for scale. Locations shown in Fig. 2.

are presumed to denote an Archaean episode of crustal extension that must have occurred between the emplacement of the orthogneisses at around 2.85–2.80 Ga (see below) and the latest (Archaean) episode of deformation at  $2748 \pm 19$  Ma as determined by Thrane & Connelly (2006).

In the south-eastern part of the Kangaatsiaq map area the orthogneisses display an overall prograde transition into brown-weathering, granulite facies, medium-grained, foliated to equigranular rocks with common migmatisation and up to centimetre-sized hypersthene porphyroblasts besides biotite and locally hornblende. This rock type is difficult to distinguish in the field from weakly compositionally layered, likewise migmatised, quartzo-feldspathic paragneiss (**q**) e.g. around the narrow Amitsoq fjord, especially where the latter rocks are not garnetiferous.

Hollis *et al.* (2006) carried out zircon U-Pb ion microprobe and laser ablation ICP-MS age determinations of two samples of amphibolite facies orthogneiss from Ikerassuaq/Langesund about 20 km east of Aasiaat and obtained ages of  $2831 \pm 23$  Ma and  $2741 \pm 53$  Ma, respectively. The former age was interpreted as the emplacement age of the magmatic precursor. Additional zircon U-Pb age data were obtained from a sample of orthogneiss collected on a small island just east of Maniitsoq. This orthogneiss has intrusive contacts into supracrustal amphibolite (Garde *et al.* 2004; see Appendix for age data). An emplacement age of at least *c.* 2810 Ma is indicated by the oldest grains, but many grains appear to have been affected by early lead loss (see Appendix).

Chemical analyses of orthogneiss obtained by Moye & Watt (2006) and from sample 467558 (Table 1) indicate that the compositions are predominantly tonalitic and locally granodioritic. The analysed samples have strongly fractionated rare-earth element (REE) patterns relative to chondrite, with strong enrichment in light REE and chondrite-normalised La/Lu ratios commonly  $>100$ .

### K- and Si-metasomatised orthogneiss (**gm**)

The orthogneiss exposed around Aasiaat and in the coastal area north-west of Nivaap Paa locally displays evidence of intense hydrothermal alteration related to brittle faults and fractures. The most intensely hydrothermally altered rocks are brick-red and largely consist of unoriented intergrowths of medium-grained quartz and red K-feldspar; superficially these rocks may look like granite.

Around Aasiaat the hydrothermal alteration is concentrated in centimetre- to decimetre-wide zones along

**Table 1. Chemical analyses of orthogneiss and granodiorite, Maniitsoq and adjacent islands**

	Tonalite	Granodiorite	
	467558 68°45.736'N 52°50.254'W	467565 68°45.047'N 52°59.460'W	467575 68°45.450'N 52°53.230'W
SiO <sub>2</sub>	68.654	70.029	71.848
TiO <sub>2</sub>	0.410	0.449	0.288
Al <sub>2</sub> O <sub>3</sub>	15.331	14.958	14.957
Fe <sub>2</sub> O <sub>3</sub> *	2.719	2.534	1.658
MnO	0.014	0.021	0.022
MgO	1.034	0.785	0.421
CaO	2.709	2.253	1.856
Na <sub>2</sub> O	5.180	4.760	4.900
K <sub>2</sub> O	2.119	2.694	2.805
P <sub>2</sub> O <sub>5</sub>	0.148	0.128	0.062
Volatiles	0.450	0.160	0.150
Sum	98.768	98.771	98.967
Sc	5.9	4.4	3.6
V	32	25	14
Cr	12	6	3
Co	16.6	16.6	16.3
Ni	8	5	3
Cu	6.2	3.6	5.5
Zn	50.7	59.7	43.2
Ga	20.1	22.4	22.1
Rb	63.3	134.1	174.7
Sr	828	429	336
Y	6.9	8.6	11.0
Zr	148.9	216.5	154.1
Nb	4.8	8.5	7.3
Cs	2.1	2.8	3.9
Ba	846	887	771
La	51.9	57.4	47.8
Ce	95.2	111.9	90.1
Pr	10.5	12.8	9.8
Nd	31.9	39.1	29.1
Sm	4.25	5.37	3.92
Eu	1.08	1.12	0.73
Gd	4.25	5.15	3.92
Tb	0.36	0.45	0.36
Dy	1.50	1.96	1.73
Ho	0.22	0.29	0.29
Er	0.63	0.81	0.88
Tm	0.08	0.11	0.14
Yb	0.45	0.60	0.93
Lu	0.07	0.09	0.17
Hf	3.5	5.3	4.0
Ta	1.3	1.1	3.5
Pb	10.6	15.5	18.0
Th	7.6	13.2	12.9
U	1.8	2.1	2.3
Total REE	202.3	237.1	189.9

Major elements (wt%) by XRF and trace elements (ppm) by ICP-MS at GEUS. See Kystol & Larsen (1999) for analytical procedures. Fe<sub>2</sub>O<sub>3</sub>\* = total Fe calculated as Fe<sub>2</sub>O<sub>3</sub>. Volatiles = loss on ignition corrected for oxygen uptake due to oxidation of iron.

N-S- and NNW-SSE-trending brittle faults and joints. The hydrothermal alteration at Nivaap Paa is much more widespread. The alteration occurs in elongate zones up to hundreds of metres wide, but due to the intensity of the alteration its spatial relationship to faults and joints is not

nearly as obvious as at Aasiaat. A brief investigation at the tip of the peninsula Nuuk north-west of Nivaap Paa (68°24.5'N, 51°05.7'W) shows a complete transition from minor hydrothermal alteration of migmatized orthogneiss along healed hairline fractures (Fig. 8A) to rocks which have undergone thorough hydrothermal alteration and complete recrystallisation into massive, equigranular, medium-grained quartz-K-feldspar rock with complex grain boundaries (Fig. 8D). The compositional change from the essentially unaltered to thoroughly altered rock is illustrated by four chemical analyses shown in Table 2. K, Rb, U and Th are strongly enriched in the most intensely altered rocks, whereas most other elements including REE are strongly depleted and Sr almost completely lost; an apparent gain in REE elements in samples 440935 and 440936 (Table 2) may be due to original compositional differences between the sampled rocks.

The hydrothermal alteration was most probably caused by circulation of magmatically heated meteoric water or sea water along fractures and joints in the uppermost crust. The hydrothermal episode has not been dated, but it is considered most likely that it was related to the development of the Cretaceous-Paleocene basalt province in West Greenland. In the map area the volcanic province is represented by basaltic sills of Grønne Ejland north of Nivaap Paa and dolerite dykes in the Aasiaat and Nivaap Paa areas (see below).

### Dioritic orthogneiss (di)

Medium-grained, hornblende- and/or biotite-bearing gneissic rocks of quartz-dioritic to dioritic composition occur as deformed sheets up to *c.* 200 m wide within the orthogneiss complex north-east of Kangaatsiaq. Due to strong deformation their contact relationships are ambiguous; there is no evidence, however, that any of the dioritic sheets found within the orthogneiss complex were emplaced as dykes. A deformed body of quartz diorite near Qasigiannugit in the adjacent Kangarsuneq map area, which has intrusive contacts against metasedimentary and metavolcanic rocks, yielded a U-Pb zircon age of 2801 ± 34 Ma interpreted as its emplacement age (Thrane & Connelly 2006).

### Granodioritic orthogneiss (gr)

Pale pink weathering, medium-grained orthogneiss of granodioritic composition is prominent in three places within the map area. Such granodioritic orthogneiss is exposed in the island group of Kigsigut / Kronprinsens Ejland about 40 km north-west of Aasiaat, on the *c.* 5 km

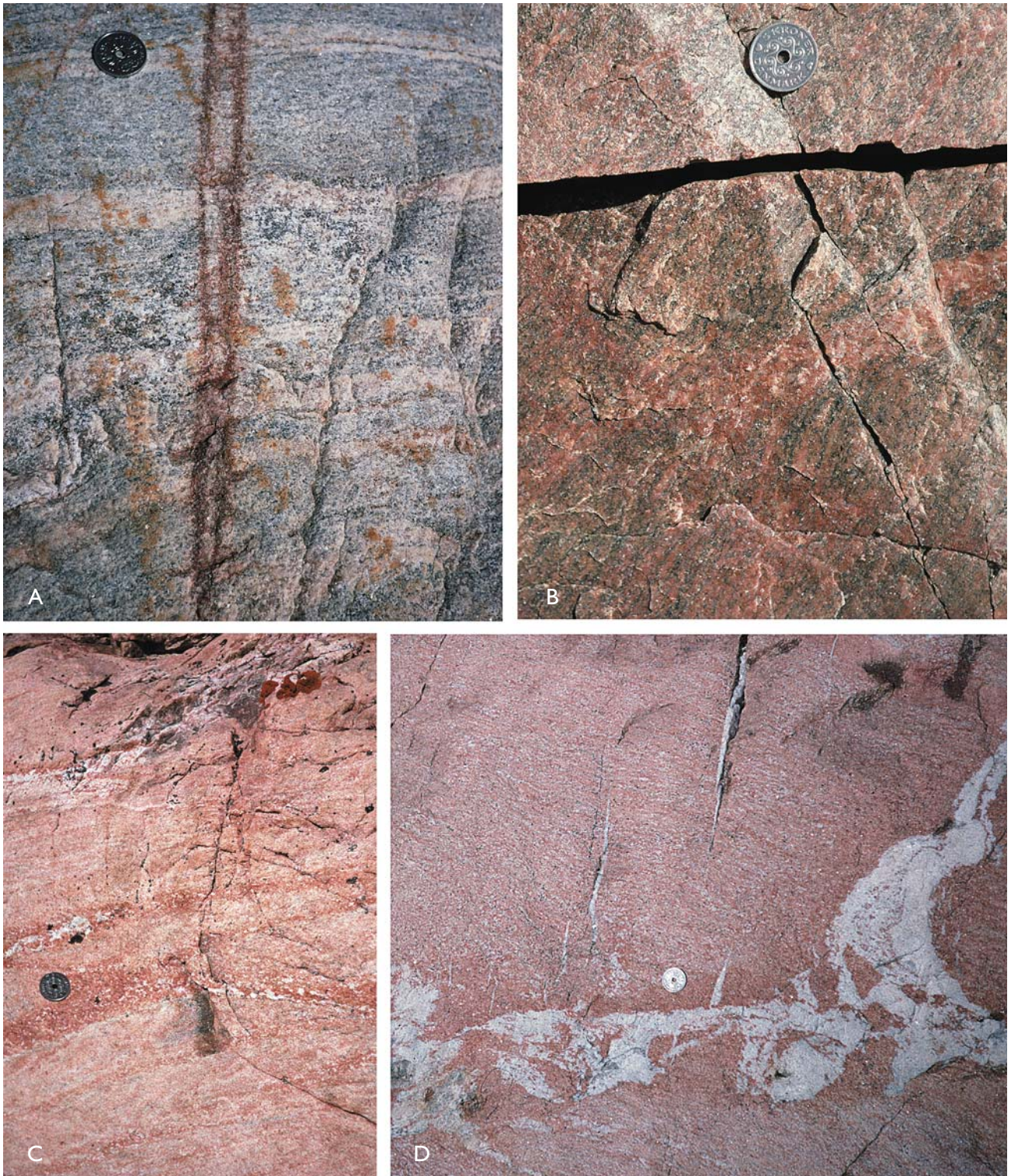


Fig. 8. Hydrothermal alteration of Archaean orthogneiss at Nuuk north of Nivaap Paa, associated with near-surface brittle faults and fractures. The alteration is interpreted as related to the Palaeogene magmatic activity at Disko Bugt (see main text). Coin is 2.8 cm in diameter. **A:** Migmatized tonalitic orthogneiss with hydrothermal alteration along hairline fractures. **B:** Partially hydrothermally altered orthogneiss. Migmatization texture still visible, and biotite present. **C:** Extensively hydrothermally altered rock, in which some parts have been completely altered to quartz – K-feldspar aggregates. **D:** Extensively hydrothermally altered rock with irregular syn-alteration quartz vein. The location is shown in Fig. 2.

**Table 2. Chemical analyses of hydrothermally altered orthogneiss, Nuuk peninsula, Nivaap Paa**

	Almost unaltered		Intensely altered	
	440934	440935	440936	440937
SiO <sub>2</sub>	70.797	74.577	75.656	75.863
TiO <sub>2</sub>	0.308	0.185	0.195	0.139
Al <sub>2</sub> O <sub>3</sub>	15.400	13.161	12.668	12.733
Fe <sub>2</sub> O <sub>3</sub> *	2.002	1.382	1.147	0.757
MnO	0.002	0.009	0.000	0.000
MgO	0.717	0.278	0.229	0.071
CaO	2.383	0.868	0.754	0.448
Na <sub>2</sub> O	5.090	3.460	3.760	4.140
K <sub>2</sub> O	2.256	5.036	4.621	4.692
P <sub>2</sub> O <sub>5</sub>	0.077	0.031	0.014	0.000
Volatiles	0.210	0.310	0.310	0.140
Sum	99.242	99.297	99.354	98.983
Sc	4.0	1.8	1.9	3.9
V	22	8	5	1
Cr	4	3	2	0
Co	13.8	19.5	15.1	19.9
Ni	5	3	2	1
Cu	3.5	8.0	3.1	1.6
Zn	42.4	25.2	35.7	12.3
Ga	21.3	17.8	17.9	21.1
Rb	65.0	133.1	162.7	244.4
Sr	389	172	105	11
Y	3.0	13.2	13.0	8.8
Zr	116.9	126.5	127.4	80.8
Nb	2.3	5.4	8.4	8.2
Cs	3.5	4.0	5.6	3.9
Ba	515	459	282	21
La	17.6	40.9	34.0	16.1
Ce	33.1	88.9	74.8	35.3
Pr	3.7	10.8	9.0	3.9
Nd	12.0	34.2	28.7	10.3
Sm	2.04	6.14	5.22	1.64
Eu	0.56	0.74	0.55	0.10
Gd	1.91	5.40	4.71	1.77
Tb	0.19	0.61	0.54	0.21
Dy	0.71	2.95	2.61	1.15
Ho	0.11	0.49	0.45	0.26
Er	0.30	1.29	1.21	0.79
Tm	0.04	0.18	0.18	0.14
Yb	0.22	0.98	1.01	0.89
Lu	0.03	0.14	0.16	0.15
Hf	3.0	3.9	3.8	3.4
Ta	1.8	1.6	3.3	1.3
Pb	6.8	21.8	20.6	25.0
Th	3.5	15.3	16.5	34.5
U	0.7	2.2	2.3	4.8
Total REE	72.5	193.7	163.0	72.7

Major elements (wt%) by XRF and trace elements (ppm) by ICP-MS at GEUS. See Kystol & Larsen (1999) for analytical procedures. Fe<sub>2</sub>O<sub>3</sub>\* = total Fe calculated as Fe<sub>2</sub>O<sub>3</sub>. Volatiles = loss on ignition corrected for oxygen uptake due to oxidation of iron.

long island of Maniitsoq and adjacent islands *c.* 5 km north-west of Aasiaat. It forms an elongate, *c.* 10 km long body underlying the Naternaq supracrustal belt in the Naternaq area. The granodiorite is commonly K-feldspar-porphyritic, and on Kronprinsens Ejland and Maniitsoq it is only weakly deformed. The granodiorite

on the latter island hosts common, flat-lying pegmatites up to a few tens of centimetres thick that are increasingly deformed towards the south. None of the three main occurrences of granodiorite display well-exposed contacts with the regional orthogneiss.

Major and trace element analysis (Table 1) and zircon U-Pb ion microprobe geochronology have been carried out on two samples from the K-feldspar-megacrystic granodiorite body which crops out on Maniitsoq and adjacent islands (Fig. 2). Sample 467565, collected on the triangular island south-west of Maniitsoq, has yielded an age of  $2771 \pm 3$  Ma (Mean Square Weighted Deviation (MSWD) = 3.3) based on the ten oldest of 18 analysed grains (see Appendix). The data obtained from sample 467575 collected on the south coast of Maniitsoq island are also of good analytical quality (see Appendix). In this sample the ages of individual zircon crystals display a wide range between *c.* 2600 and 2800 Ma. The oldest grains, which have low U and Th contents, point to a minimum age of emplacement of about 2750 Ma, consistent with the age data from sample 467565. The younger grains are U- and Th-rich (typically with U and Th contents around 1000 and 500 ppm, respectively) and are considered likely to have undergone substantial early lead loss (see Appendix).

### Granite (g)

Several large bodies of white, pink and pale red, medium- to coarse-grained, K-feldspar-porphyritic biotite granite up to a few kilometres across occur within the map region. Similar granite also occurs as smaller sheets and metre- to centimetre-scale veins. The granite bodies are generally less deformed than their orthogneiss hosts. Field observations of gradational transitions between migmatitic veins in tonalitic orthogneiss and massive granite suggest that the granite has been derived from adjacent tonalitic–granodioritic orthogneiss (Fig 9). The three largest occurrences are the Kangaatsiaq granite east of Kangaatsiaq (Moyen & Watt 2006) and two bodies south of Nivaap Sullua *c.* 20 km west of Ikamiut and south-east of Alanngorsuup Imaa (Fig. 2). The Kangaatsiaq granite is pink, coarse-grained and K-feldspar-porphyritic, and displays a strong rodding lineation and schistosity (L to L>S tectonic fabric). It was emplaced into a series of basic to intermediate metavolcanic and pelitic rocks and subsequently folded into a complex synform a few kilometres wide (Moyen & Watt 2006, fig. 2). The granite west of Ikamiut, which is located within the hinge zone of a large antiform, was described by Hollis *et al.* (2006). It is porphyritic and holds a weak tectonic fabric, much weaker than found in the surrounding supracrustal rocks and orthogneisses.

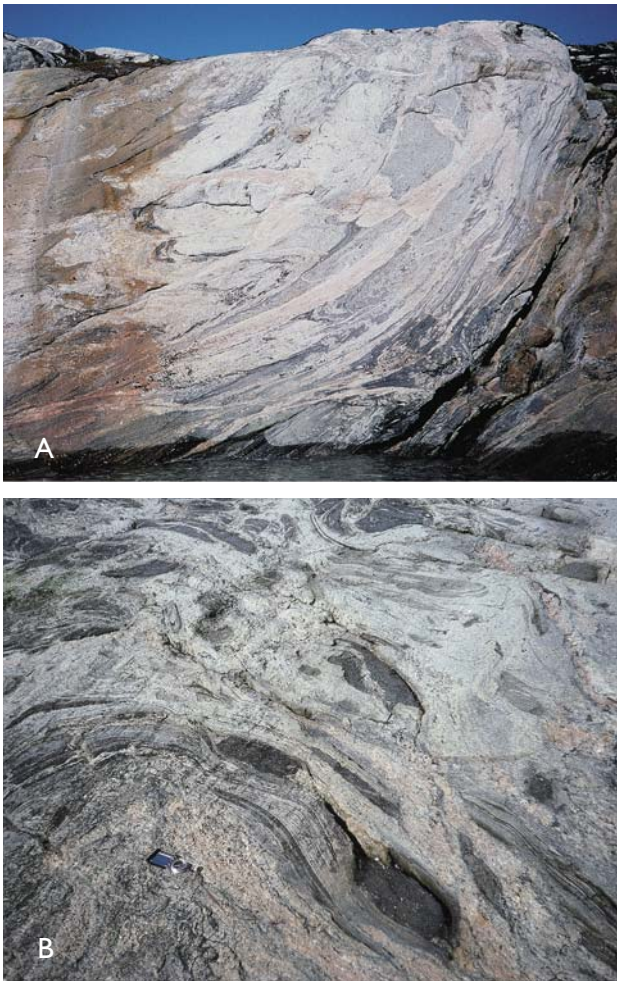


Fig. 9. Late-kinematic granite sheets and veins in the hinge zone and flank of a major Archaean fold system at Saqqarput. The granite sheets and veins cut grey orthogneiss with xenoliths of homogeneous, medium-grained metagabbro. A: Approximately 2 m wide outcrop in splash zone on the north side of outer Saqqarput. B: Head of Saqqarput. Compass for scale. Locations shown in Fig. 2.

The position of the granite west of Ikamiut in an antiformal hinge zone and its relatively undeformed nature suggest it was emplaced late in the Archaean deformation history after the main fabric-forming events. The field observations suggesting that the granite bodies have been derived by partial melting of orthogneisses are supported by the chemical composition of the Kangaatsiaq granite, which is slightly metaluminous with low Ni and Cr contents and low Mg/Fe ratios and moderate Rb, Sr and Ba contents. The REE concentrations are slightly higher than in the regional orthogneiss. The REE patterns in chondrite-normalised diagrams are similar to those of the regional orthogneiss except for variable negative Eu anomalies which point to retention of plagioclase in the granite source (Moyen & Watt 2006).

### Granitic and pegmatitic veins (p)

The pegmatite symbols shown in full red colour on the maps denote areas with decimetre- to metre-sized and occasionally thicker sheets of variably deformed pegmatite of presumed Archaean age, as well as areas with abundant migmatisation and local, partial melt veins centimetres to decimetres thick, which have been visibly separated from their source. The pegmatites are of the simple type with about equal proportions of quartz, K-feldspar and sodic plagioclase, as well as minor biotite. Centimetre- to metre-thick veins of late-kinematic granite occur e.g. at Saqqarput, where they commonly form small discordant bodies in hinge zones of folds (Fig. 9A) and thin sheets and veins subparallel to the deformed flanks of the same generation of folds (Fig. 9B). A zircon  $^{207}\text{Pb}/^{206}\text{Pb}$  age of  $2748 \pm 19$  Ma age was obtained from a late-kinematic granite on the flank of one of these folds (Thrane & Connelly 2006), proving the Archaean age of the regional deformation in the southern part of the Aasiaat domain.

The extensive biotite-garnet-sillimanite schist southwest of Nivaap Paa in the Ikamiut map area has been subject to widespread partial melting resulting in centimetre- to metre-sized schlieren and veins of white, heterogeneous, coarse-grained, garnet-bearing granite grading into pegmatite. The partial melting event in this area has not been dated. However, age determination of metamorphic rims on zircon grains from an adjacent metasedimentary rock collected on the south coast of Nivaap Paa suggests that the area underwent high-grade metamorphism at *c.* 2740–2700 Ma (Hollis *et al.* 2006). It is therefore considered most likely that the partial melting of the biotite-garnet-sillimanite schist was Archaean and broadly contemporaneous with partial melting in the southern part of the Aasiaat domain (and thus unrelated to Nagssugtoqidian thermal reworking, see later).

### Archaean supracrustal and related intrusive rocks: main components and relationships with orthogneiss

Like in other Archaean regions within the Nagssugtoqidian orogen, and in the North Atlantic craton farther south (Windley & Garde 2009), the orthogneisses in the map area are intercalated with supracrustal associations of (meta) volcanic, intrusive and sedimentary rocks. In low-strain areas such as hinge zones of Archaean folds the orthogneiss precursors can be seen to have intruded into the supracrustal rocks, and a majority of the supracrustal belts are thus likely to be older than the orthogneisses.

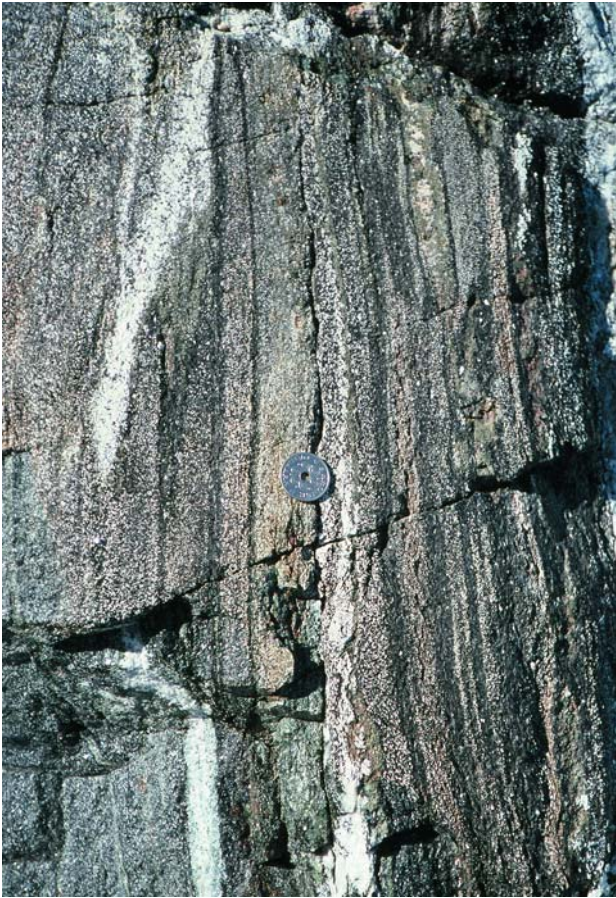


Fig. 10. Heterogeneous amphibolite, possibly of tuffaceous origin, with centimetre-scale compositional layering and widely spaced strings of hypersthene. Coin for scale (d = 2.8 cm). South side of outer Saqqarput (see Fig. 2).

Heterogeneous, fine-grained mafic amphibolite of presumed volcanic origin (locally associated with layered metagabbro) and biotite schist ( $\pm$  muscovite, garnet and/or sillimanite) are the two most widespread rock types and commonly occur together. Kalsbeek & Taylor (1999) obtained a Palaeoproterozoic Rb-Sr whole-rock age from metasedimentary rocks at Ikamiut, whereas their extrapolation backward in the Sr evolution diagram points to a depositional age at around 2.8 Ga.

The occurrences of quartzo-feldspathic paragneiss in the south-east of the Kangaatsiaq map area are not associated with amphibolite except in a synform on the south coast of Arfersiorfik at 68°07'N. The structurally lowest supracrustal rocks in this synform are quartzite and marble a few metres thick, overlain by quartzo-feldspathic paragneiss and fine-grained amphibolite in the core of the synform. During the field work for the Kangaatsiaq map sheet no depositional unconformity between the quartzite and the underlying orthogneiss was recognised. The contact appears to be tectonic but was not scrutinised along its entire length.

### Amphibolite (a)

The largest, more or less coherent outcrops of amphibolite occur in southern Naternaq and around Arfersiorfik in the Kangaatsiaq map area and outline a broad, more or less continuous arc, which is more than 40 km long and comprises refolded, tight to isoclinal overturned folds. Fine-grained, heterogeneous amphibolite with a strong planar and linear tectonic fabric and an irregular deformed, centimetre- to decimetre-scale network of veinlets with diopside, calcic plagioclase and locally garnet and/or calcite is most common. Other outcrops display centimetre-scale compositional layering but are devoid of calc-silicate minerals (Fig. 10), and may be of tuffaceous origin. Horizons of homogeneous amphibolite up to several metres thick are also common. Møyen & Watt (2006) presented geochemical data for seven samples of fine-grained, mafic amphibolite collected north-east of Kangaatsiaq and concluded that the amphibolite is tholeiitic and MORB-like, with completely flat chondrite-normalised REE patterns at about 10  $\times$  chondrite.

The fine-grained, heterogeneous, calc-silicate-bearing amphibolite is interpreted as volcanic in origin, most likely pillow lava or pillow breccia. The homogeneous varieties of fine-grained amphibolite may represent former hypabyssal sills and/or flows.

Successions up to 10–20 m thick of fine-grained, grey hornblende-plagioclase-biotite rocks displaying well-defined, planar compositional, centimetre-thick layering are common and frequently associated with ordinary mafic amphibolite. They have typically been given field labels such as 'intermediate amphibolite' or 'grey amphibolite', and have andesitic compositions. Locally volcanoclastic rocks with centimetre-scale angular, felsic clasts in a fine-grained, darker matrix have also been found, e.g. on the western side of the small island between the islands of Qeqertarsuaq and Naajat (Fig. 11C). These rocks are interpreted as intermediate volcanic breccia, tuff and/or tuffite. Some of these successions also comprise zones rich in garnet and biotite but with low feldspar contents (Fig. 11A–B). Similar Archaean garnet-rich parageneses devoid of feldspar are known e.g. from metamorphosed intermediate tuffs or tuffites in the Godthåbsfjord region that have been affected by intense synvolcanic hydrothermal alteration (e.g. Garde *et al.* 2007b; Garde 2008).

### Metagabbro (ai)

Medium-grained hornblende-plagioclase metagabbro, locally with centimetre-sized, euhedral hornblende and/or plagioclase megacrysts, is sometimes intercalated within the fine-grained amphibolite or crops out within the orthogneiss as discrete bodies with tectonic or tec-

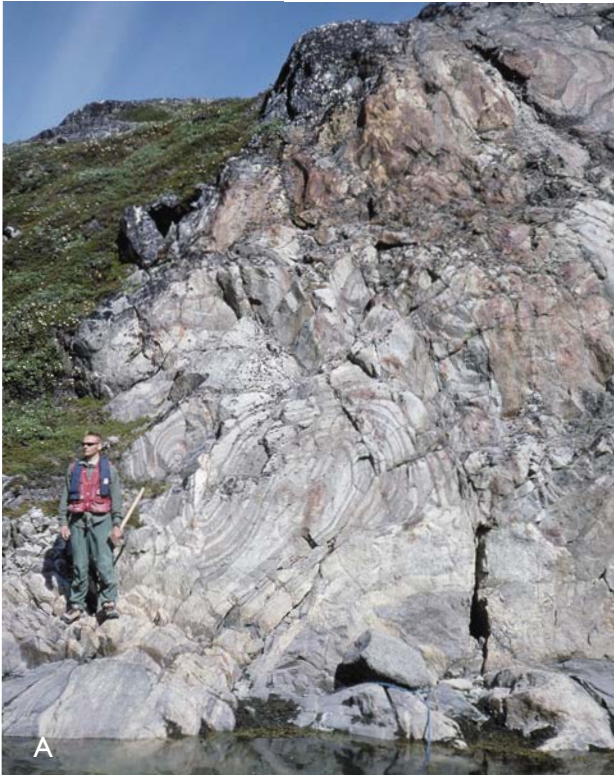


Fig. 11. **A, B:** Layered and tightly folded, fine-grained rock of intermediate composition (metatuff?) with a garnet- and biotite-rich zone, possibly due to synvolcanic hydrothermal alteration. South coast of Tunorsuaq with person for scale. **B:** Enlarged part of Fig. 11A just right of person, *c.* 1 m across. Location shown in Fig. 2.

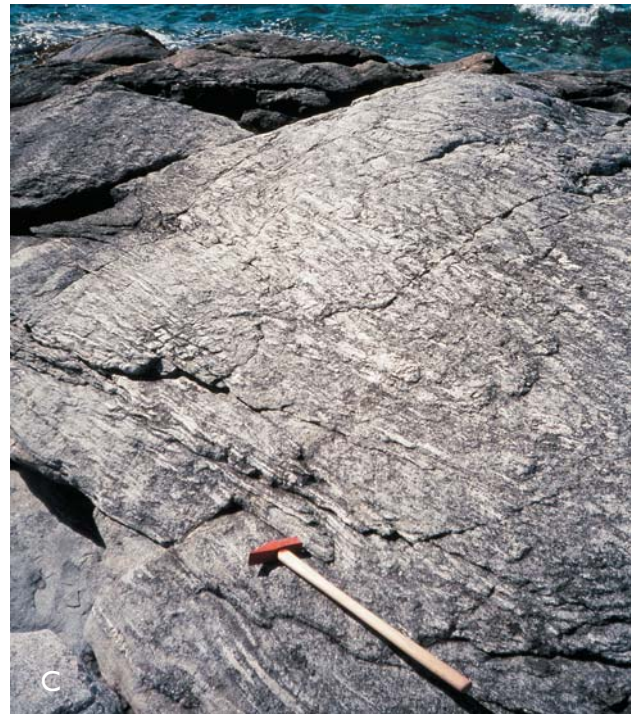


Fig. 11. **C:** Volcaniclastic texture in biotite-hornblende-plagioclase rock of intermediate composition. West side of small island between Qeqertarsuaq and Naajat islands. Location shown in Fig. 2.

tonised margins. A medium- to coarse-grained metagabbro body *c.* 2 km in diameter at Ataneq also comprises coarse-grained leucogabbro locally grading into anorthosite. The (meta) gabbroic and associated rocks are considered to be an integral part of the supracrustal association *s.l.* which predates the orthogneisses.

On the island west of the abandoned settlement Ikerasak in the south-western corner of the Kangaatsiaq map area, within the granulite facies part of the Aasiaat domain, occurs a tightly folded body of metagabbro with a stratigraphic thickness of several hundred metres. The metagabbro is part of a supracrustal association that also comprises fine-grained, heterogeneous amphibolite and biotite schist. It has not been mapped in detail, but according to a few observations along the coasts of the island it consists of medium-grained rocks with variable proportions of hornblende, orthopyroxene, iron oxide and plagioclase, which commonly display centimetre- to decimetre-scale magmatic layering. Another much smaller sheet of metagabbro occurs 3 km east of Ikerasak. It is more than 50 m thick and displays well-exposed, rhythmic, magmatic, centimetre-thick layering (Fig. 12). Its contact relations with the orthogneiss are not known; it may be a raft of the former body.



Fig. 12. A, B: Archaean layered (meta)gabbro associated with meta-volcanic amphibolite and mica schist (not shown) and metamorphosed under granulite facies conditions. Compass for scale in Fig. 12B. Location 3 km east of the abandoned village Ikerasak at 68°N (see Fig. 2).

### Anorthosite and leucogabbro (an)

Coarse-grained anorthosite with calcic plagioclase of the ‘Fiskenæsset type’ (Myers 1985) has been observed on the islands of Saattut and Upernivik at Nivaap Paa associated with coarse-grained hornblende leucogabbro. On Saattut itself the anorthosite–leucogabbro displays a tectonic or tectonised magmatic contact against biotite schist, whereas no other rock types (and thus no contacts) have been observed on Upernivik or its adjacent skerries. South of Saattut a train of intensely deformed anorthosite inclusions is sandwiched between orthogneiss and metasedimentary rocks. Intensely deformed anorthosite–leucogabbro is also found in a *c.* 2 km large body of metagabbro at Tulukaat Tasersuat north of Ataneq (Fig. 13).

### Ultrabasic rocks (ub)

Ultrabasic rocks only form a tiny proportion of the map area, mainly as intensely deformed, variably serpen-



Fig. 13. Intensely deformed anorthosite–leucogabbro associated with a *c.* 2 km large body of metagabbro, and cut by subhorizontal granitic vein. 2.8 cm coin for scale. Inlet of Tulukaat Tasersuat north of Ataneq (see Fig. 2).

tinised, metre-sized layers and lenses of medium-grained, olivine- and pyroxene-rich rocks. The ultrabasic rocks occur within or adjacent to amphibolite e.g. on an elongate island 7 km north-east of Aasiaat, and form trains of tectonic lenses in orthogneiss e.g. north of inner Saqqarput and south of Arfersiorfik. None of them have been studied in detail.

### Biotite schist and paragneiss ± garnet and/or sillimanite (s)

The second most widespread Archaean supracrustal lithology after the fine-grained amphibolite is 2–3 mm-grained, compositionally layered biotite schist ± garnet-, muscovite and/or sillimanite. The biotite schist is commonly interlayered with the amphibolite varying from tens to hundreds of metres. The biotite schist may grade into quartzo-feldspathic paragneiss ± garnet, and e.g. in the Ikamiut area grades into pale, siliceous paragneiss (q). Biotite schist also commonly forms elongate xenoliths in adjacent orthogneiss, indicating that at least some schist occurrences are older than the latter. As mentioned under the heading ‘Granitic and pegmatitic veins’, partial melting of biotite schist is widespread in some areas and particularly prominent south-west of Nivaap Paa.

Sillimanite is relatively common in some areas and almost invariably occurs within distinct layers a few centimetres apart as evenly scattered, blocky, centimetre-sized aggregates. The sillimanite aggregates are roughly lozenge-shaped where deformation is not intense, and are interpreted as pseudomorphs after andalusite. The repetitive distribution of these aggregates within regularly spaced layers may suggest that these rocks were originally deposited from density currents.

Medium-grained quartzo-feldspathic paragneiss, commonly garnet-bearing and commonly grading into biotite schist, forms large outcrops in the south-eastern part of the map area especially around Amitsoq. Due to deformation and granulite facies metamorphism, the exact boundaries of these rocks are difficult to determine, and their contact relationship with the orthogneisses has not been established.

Hollis *et al.* (2006) performed a zircon U-Pb ion microprobe and Pb-Pb laser ablation ICP-MS age determination of a gneissic quartzo-feldspathic rock from the Ikamiut area. They obtained a tight cluster of ICP-MS ages close to 2800 Ma from cores of individual zircon grains with igneous-type oscillatory zonation, which thus represent the maximum age of deposition. This overlaps with the age of an orthogneiss from the same area mentioned above (see the section 'Archaean crustal evolution').

Moyen & Watt (2006) described aluminous metapelite and layered biotite gneiss north-east of Kangaatsiaq and used major and trace element geochemical data to discuss their origin; as these particular rocks are not sufficiently voluminous to be shown separately on the map, they are both comprised in the unit of quartzo-feldspathic paragneiss (**q**). Moyen & Watt (2006) concluded that the composition of the aluminous metapelites consistently points to a depositional setting in a continental or oceanic arc with a volcanic component in the source. Relatively high Ni, Cr and heavy REE contents preclude an origin solely from continental rocks such as TTG gneisses. This conclusion is in agreement with the field characteristics of the biotite schists and their contact relationships with adjacent rocks. The layered biotite gneiss yielded an ambiguous major and trace element geochemical signature. According to Moyen & Watt (2006) the layered biotite gneiss may either be interpreted as a felsic volcanic rock (their preferred interpretation) or as a clastic sedimentary rock.

### Quartzo-feldspathic paragneiss (**q**)

Quartzo-feldspathic and/or siliceous biotite paragneiss has been mapped in three areas: south and east of Kangaatsiaq, around the narrow fjord of Ataneq in the southern part of the Kangaatsiaq map area where the rocks are more micaceous and occasionally associated with amphi-

bolite (and shown as mica schists on the map), and at Nivaap Paa in the eastern part of the Ikamiut map area where siliceous paragneiss grades into biotite schist. The rocks in the latter area shown as quartzo-feldspathic paragneiss on the map mainly comprise a distinct, compact, pale-greyish yellow to almost white, siliceous lithology which is locally garnet-bearing. It is distinguished from the biotite schist by its more quartz-rich and mica-poor composition, and is often difficult to distinguish from the regional orthogneiss. The quartzo-feldspathic paragneiss has SiO<sub>2</sub> contents between about 60 and 74 wt%, and its overall chemical composition is comparable to orthogneiss (Hollis *et al.* 2006; Moyen & Watt 2006). It has intermediate Rb, Sr and Ba contents, low base metal contents, and steep chondrite-normalised REE patterns with very low heavy REE. It may either represent immature sediment derived from TTG orthogneisses or redeposited felsic volcanic rocks.

Thrane & Connelly (2006) obtained a cluster of laser ICP-MS <sup>207</sup>Pb/<sup>206</sup>Pb ages around 2850 Ma from detrital zircon grains with igneous zonation in a quartz-rich metasedimentary rock at the head of Amitsoq. Accordingly the sediment was deposited after 2850 Ma. The age maximum is comparable to the age of the surrounding orthogneisses (see 'Archaean crustal evolution'). Detrital zircon grains in another sample collected within the area described by Moyen & Watt (2006) north-east of Kangaatsiaq was also dated with the same method. A range of individual dates from 3200 Ma (only one grain) to 2595 Ma was obtained, with a peak around 2850 Ma which according to Thrane & Connelly (2006) is the probable maximum depositional age as well as the age of the main source; the younger grains are considered likely to have undergone substantial, early lead loss.

### Marble and calcareous rocks (**m**)

Two very small occurrences of marble and calc-silicate rocks have been found just east of Maniitsoq island (north of Aasiaat) and on the south coast of Arfersiorfik near the south-eastern map boundary. Medium-grained, equigranular calcite marble locally forms layers up to *c.* 20 cm thick interspersed with more voluminous diopside-rich calc-silicate rocks. The marble and calcareous horizons are in turn interstratified with quartzo-feldspathic metasedimentary rocks.

# Palaeoproterozoic map units

## Naternaq supracrustal belt at Naternaq/Lersletten: main components and structure

The *c.* 20 km long and up to 4 km wide, intensely deformed Naternaq supracrustal belt is the only large occurrence of metavolcanic and metasedimentary rocks of known Palaeoproterozoic age (Fig. 14; Østergaard *et al.* 2002; Garde & Hollis 2010). Most of the belt occurs in the north-eastern part of the Kangaatsiaq map area; its northernmost part within the Ikamiut map area appears under the heading ‘West of Kuussuup Qinnua’ on the latter map. The Naternaq supracrustal belt shows up on the aeromagnetic map as an area with low total magnetic intensity (Fig. 4, right side of arrow). It mainly consists of fine-grained amphibolite and siliceous to aluminous mica schist, besides volumetrically minor calcareous and volcanogenic-exhalative rocks. Only some parts of the belt have been mapped in detail, and accordingly it may not yet be fully understood (see below). The belt was previously considered to be of Archaean age, but detrital zircon age data from a fine-grained muscovite-sillimanite schist in its southern part have yielded a maximum depositional age of  $1904 \pm 8$  Ma (Thrane & Connelly 2006,

including data by the present authors). This depositional age is compatible with derivation from a hypothetical volcanic arc associated with the 1921–1885 Ma Arfersiorfik intrusive suite in the central Nagssugtoqidian orogen. The southern part of the Naternaq supracrustal belt hosts a massive sulphide deposit, which was investigated by the company Kryolitselskabet Øresund A/S in the 1960s (see section on economic geology).

With its Palaeoproterozoic age the Naternaq supracrustal belt is an important structural marker, resting on the Archaean basement above a presumed tectonic contact. It comprises an overturned, asymmetrical syncline (F1) with an intense planar fabric (S1), which has been refolded into a large V-shaped body. Its NNE–SSW-trending western limb delineates a major, map-scale structural discordance against the underlying Archaean orthogneiss with its narrow, WNW-trending metavolcanic amphibolite belts and flat-lying lineations and fold axes. The discordance is conspicuous on both aeromagnetic and geological maps (Figs 4, 14). The contact itself is only exposed in the southern hinge zone of the Naternaq belt and along part of the southern limb of its main

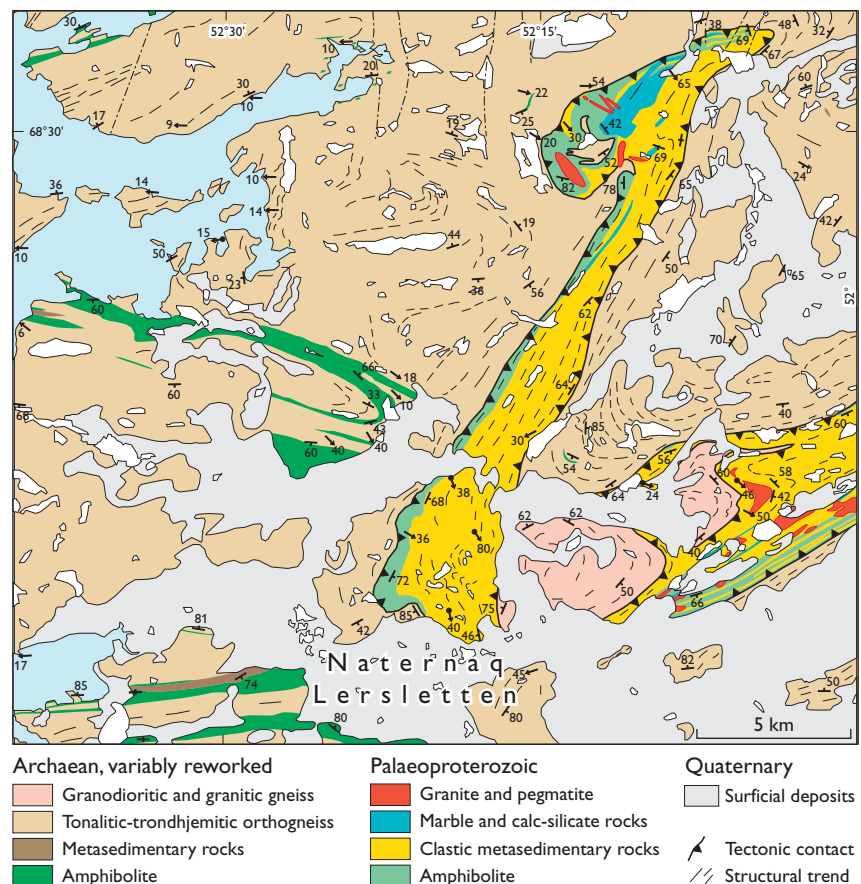


Fig. 14. Simplified geological map of the Palaeoproterozoic, multiply folded Naternaq supracrustal belt, superseding a previous map in Østergaard *et al.* (2002). Note the structural discordance along the left flank of the belt against the underlying, E–W-trending Archaean rocks. See the main text for details and discussion.

syncline. It is intensely deformed in both areas and is almost certainly a refolded thrust.

The main F1 syncline and its intense S1 fabric have been folded into its present V-shape by a second tight, kilometre-scale, SE-plunging syncline (F2). Several smaller upright to overturned, SE-plunging folds in the south-western part of the belt are interpreted as parasitic to this major F2 fold. These folds commonly display a strong SE-plunging mineral and extension lineation (see below), but an axial planar fabric to the F2 folds is rarely developed. Another group of F2 folds occur in the northern part of the belt, east of the rectangular lake with the elongate island. In both areas the hinge zones of the F2 folds commonly contain irregular, tourmaline-bearing pegmatites which may grade into coarse-grained, very leucocratic granite (**gp**, see below). The northern F2 folds and their lineations have been reoriented by an open, E–W-trending F3 fold with a subhorizontal axis. The prominent isoclinal synform fold at the northern termination of the Naternaq supracrustal belt folds the intense S1 fabric as well as the underlying orthogneiss, and is likewise interpreted as a F3 fold (the steep plunge of the fold axis may be inherited from a previous F1 or F2 fold).

Assuming that this correlation of deformation phases is correct, the strain associated with the F3 folding strongly increases towards the north and may thus be contemporaneous with the intense regional ENE-trending fabric that is prominent in most of the Ikamiut map area. The regional implications of the structural description and interpretation outlined above are addressed later in the section ‘Palaeoproterozoic tectonic evolution and plate-tectonic model’.

### **Amphibolite (na, na<sub>2</sub>)**

Amphibolite mainly occurs as a *c.* 200–400 m thick belt along the outer periphery of the Naternaq supracrustal belt, which is intercalated with thinner strata of mica schist (Østergaard *et al.* 2002). Only small pockets of amphibolite have been preserved on the northern flank of the southern, E–W-trending part of the main syncline, along the tectonic contact with the orthogneisses. The amphibolite is mostly a very fine-grained hornblende-plagioclase rock which is commonly very schistose and/or intensely lineated, especially along the outer margin of the belt. Minor quartz and biotite are common, and locally garnet is present. Some localities display 1–5 cm long plagioclase aggregates. The amphibolite very commonly contains irregular, interconnected calc-silicate layers and lenses up to a few centimetres thick, which are more or less conformable with the main foliation. Calc-silicate layers up to *c.* 20 cm thick and tens of metres long have locally also been observed.

The fine-grained amphibolite with calc-silicates is interpreted as former pillow lava and/or pillow breccia. Medium-grained, grey, homogeneous, plagioclase-rich, biotite-bearing amphibolite of andesitic composition locally occurs, as well as hornblende-quartz rocks of presumed hydrothermal origin. Small bodies of medium-grained, variably foliated hornblende- or plagioclase-porphyroblastic amphibolite are interpreted as intrusive in origin.

### **Biotite ± muscovite schist, commonly with garnet, staurolite and/or sillimanite (ns)**

The largest part of the Naternaq supracrustal belt is comprised of fine-grained, pelitic to siliceous biotite ± muscovite schist. The most siliceous varieties are generally light grey to light brown and commonly appear massive without much apparent lithological variation. No primary structures have been observed within them. In some places these rocks contain up to centimetre-sized, blocky aggregates of sillimanite after andalusite. Garnet-rich horizons are common adjacent to amphibolite contacts. Layers of fine- to medium-grained garnet-mica schist ranging from centimetres to many metres in thickness, commonly sillimanite- and locally staurolite-bearing (Fig. 15A), are intercalated with both siliceous schist and amphibolite; these rocks mostly display a strong penetrative S or LS fabric. In some areas they contain local, quartzo-feldspathic, centimetre-thick melt veins.

The biotite ± muscovite schist may in part be of volcanic origin, most likely derived from acid tuff or tuffite.

### **Marble and calc-silicate rocks (c), and volcanogenic-exhalative horizons with chert and sulphidic rocks (v)**

In the southern and north-western parts of the Naternaq supracrustal belt the peripheral amphibolite is succeeded inwards/upwards by an irregular, generally intensely deformed sequence of marble, minor carbonate- and oxide-facies banded iron formation and cherty exhalites, and local semi-massive to massive sulphides. Detailed mapping by Østergaard *et al.* (2002) showed that a single original sequence has been repeated by folding so that it crops out as three geographically separate belts in some areas.

The up to *c.* 100 m thick occurrences within the Naternaq belt shown as marble on the Kangaatsiaq and Ikamiut map sheets mainly consist of impure, greyish to brownish weathering, fine-grained dolomitic marble, commonly with centimetre- to decimetre-thick intercalations of calcite marble and calc-silicate rocks dominated



Fig. 15. Palaeoproterozoic rocks in the southern part of the Nater-naq supracrustal belt. A: Staurolite schist; 2.8 cm coin for scale. B: Carbonate facies banded iron formation just outside the map area at 68°24.6'N, 51°54.6'E; coin for scale. C: Tourmaline pegmatite; the largest tourmaline crystals are about 5 cm across. The locations of A and C shown in Fig. 2.

by tremolite/actinolite + diopside ± dolomite and late talc. The lack of forsterite and the presence of sillimanite in adjacent pelitic rocks suggest P-T conditions of approximately 650 ± 50°C at 4.5 ± 0.5 kbar; tremolite/actinolite may have grown during decreasing temperature. Carbonate-facies banded iron formation forms sporadic, 0.5–1 m thick layers on the south-eastern fold

flank along strike of the dolomite marble, and consists of alternating centimetre-thick layers of dolomite, magnetite, siderite, quartz, and calc-silicate minerals (Fig. 15B; Østergaard *et al.* 2002).

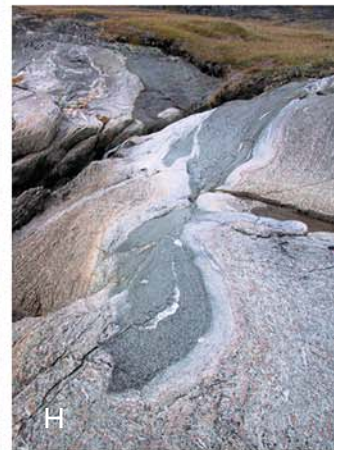
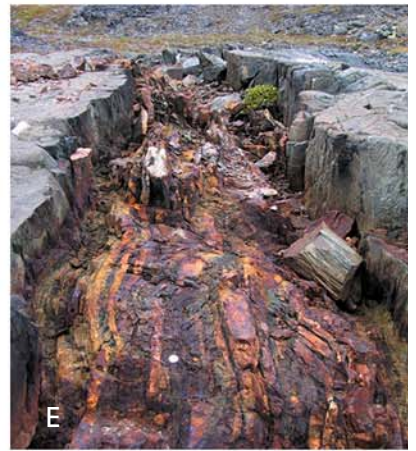
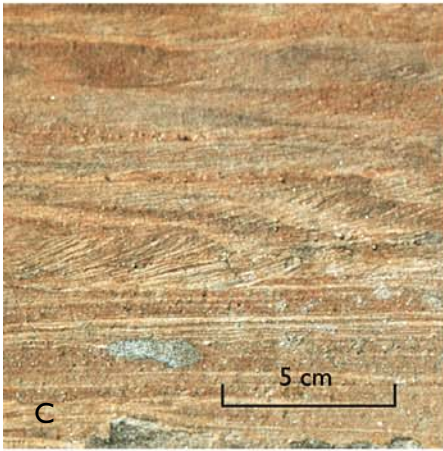
A range of conformable horizons of very fine-grained siliceous and sulphidic rocks associated with amphibolite and/or marble were interpreted by Østergaard *et al.* (2002) as volcanogenic-exhalitic rocks. Light grey, finely laminated cherty rocks predominate and usually contain up to *c.* 20% dark, very fine-grained sulphidic seams. A fine lamination of presumed chemical sedimentary origin has been destroyed in most places by intense hydrothermal alteration and impregnation with iron sulphides. Seams of fine-grained dolomite and micaceous sediment are commonly intercalated with the mineralised cherty layers, resulting in heterogeneous, rusty weathering outcrops. The largest semi-massive to massive, pyrrhotite-rich sulphide mineralised zones are located just east of the map boundary (see Østergaard *et al.* 2002). Disseminated sulphides are common in the host rocks adjacent to the semi-massive and massive sulphide occurrences.

### Metavolcanic and metasedimentary rocks on Isuamiut–Qaqqarsuatsiaq and Equutiit Killiat islands and Hunde Ejlande north-east and north of Aasiaat

A large variety of spectacular Palaeoproterozoic meta-volcanic and metasedimentary rocks crop out on the Isuamiut–Qaqqarsuatsiaq and Equutiit Killiat islands north-east of Aasiaat. These islands were first studied by Ellitsgaard-Rasmussen (1954), who published a map and a detailed description of metamorphic parageneses and the main structures. A short account by Garde *et al.* (2004) presented previously unrecognised primary volcanic and sedimentary features such as pillow structures and graded bedding.

The latter authors presumed that the rocks on these islands were Archaean, based on correlation along strike with fine-grained amphibolite and pelitic metasedimentary rocks on other small islands farther west, where Archaean orthogneiss has intruded the amphibolite (Garde *et al.* 2004). However, Garde & Hollis (2010) have demonstrated that the Isuamiut–Qaqqarsuatsiaq and Equutiit Killiat islands are of Palaeoproterozoic age, as detrital zircon from a metasedimentary rock have yielded a maximum deposition age of *c.* 1850 Ma.

Mafic pillow lava and sills, black manganiferous chlorite schist, chert, banded iron formation, graded aluminous schist and siliceous sandstone are the main components. The rocks are mostly excellently preserved at low to intermediate amphibolite facies grade, mainly



attributed to contact metamorphism (Garde & Hollis 2010). The rocks generally possess a single weak to moderate cleavage, which is axial planar to upright to overturned, S-plunging folds ranging from metres to hundreds of metres in wavelength and amplitude. Garde & Hollis (2010) interpreted these rocks as representing an ocean-floor assemblage on Isuamiut–Qaqqarsuatsiaq (Fig. 16A–E) and a buried spreading ridge adjacent to an arc trench on Equutiit Killiat (Fig. 16F–K). Similar undated rocks on Hunde Ejlände are tentatively assigned to the same Palaeoproterozoic association.

### Greenstone: pillow lava ( $\pi$ ) and sill complex ( $na_1$ , $na_3$ ); garnet-bearing greenstone ( $ng$ )

Fine-grained mafic pillow lava and sills (Figs 16A, 16H, 16K), typically comprising massive actinolite, albite and epidote  $\pm$  garnet, are the most widespread rocks on the Isuamiut–Qaqqarsuatsiaq islands, alternating with layers of chloritic schist. At the contacts the sills preserve chilled margins, which grade into more massive and slightly coarser-grained actinolite-albite rocks that dominate the outcrops of mafic rocks. Fine-grained mafic sills with chilled intrusive contacts into aluminous metatur-

bidites are abundant on the Equutiit Killiat islands (see below). The greenstone succession on south-eastern Hunde Ejlände also comprises two garnet-bearing horizons, each about 50 m thick.

### Staurolite-andalusite-muscovite-biotite-garnet schist ( $ss_1$ , $ss_3$ )

Aluminous andalusite-staurolite  $\pm$  garnet schist forms most of the Equutiit Killiat islands, along with mafic sills. The schist displays more or less ubiquitous and well-preserved graded bedding (Fig. 16G), locally with finely laminated beds and local climbing ripple marks (Figs 16F, 16J). Where observed, the sedimentary younging is structurally upward. Mafic sills are abundant (Figs 16H, 16K, see above). The sandy bases of graded beds are quartzo-feldspathic and biotite-bearing; centimetre-sized staurolite and biotite porphyroblasts occur in the middle parts, and the aluminous tops host subhedral andalusite crystals up to *c.* 5 cm in size (Fig. 16G). At the contacts to the sills the schists display ubiquitous recrystallised and apparently metasomatised reaction rims up to about 10 cm wide (Figs 16H, 16K).

### Chlorite schist ( $cs$ ) with intercalations of sandstone ( $mm$ ), chert ( $cq$ ), banded iron formation and calcareous rocks

Dark, fine-grained, relatively siliceous chlorite-garnet-biotite  $\pm$  muscovite schist with very fine-grained disseminated graphite (Fig. 16B) is widespread on the Isuamiut–Qaqqarsuatsiaq islands, intercalated with greenstone of in- and extrusive origin. The chloritic schist is manganese-rich (Garde & Hollis 2010). Local beds of quartz-rich sandstone occur within the dark chloritic schist and typically range from a few centimetres to a few decimetres in thickness (Fig. 16B); a sandstone unit up to 10 m thick was observed at the western end of the island northwest of Qaqqarsuatsiaq. Larger exposures of quartz-rich sandstone and arkose occur in northern Hunde Ejlände. The chloritic schist locally preserves centimetre-thick, graded bedding and ripple marks (Fig. 16C). In some places the schist is interlayered with finely laminated, fine- to medium-grained actinolite-albite  $\pm$  garnet-bearing siliceous rocks less than 1 m thick, which are interpreted as metamorphosed tuffs.

On the Isuamiut–Qaqqarsuatsiaq islands there are also horizons and elongate lenses up to a few metres thick of chert, jasper (Fig. 16D), manganese-rich banded iron formation (Fig. 16E) and iron-rich carbonate rocks with actinolite and locally diopside. These rocks are interstratified with the chlorite schist and greenstones.

#### *Facing page:*

Fig. 16. Distinctive ocean-floor and arc trench assemblages at middle amphibolite facies north-east of Aasiaat (from Garde & Hollis 2010). Coin for scale is 2.8 cm across. Pillow lava, siliceous chlorite schist, chert and banded iron formation on the Isuamiut–Qaqqarsuatsiaq islands (A–E) are interpreted as volcanic and hydrothermal ocean-floor deposits and (hemi)pelagic sediments. Terrigenous graded and laminated clastic deposits with numerous intercalated sills on the Equutiit Killiat islands (F–K) are interpreted as representing a buried spreading ridge receiving terrigenous input in the form of distal turbidites. The directions of younging in the metasedimentary rocks are right way up. **A:** Pillow lava, northern Isuamiut. **B:** Fine-grained chloritic schist with graded sandstone bed, south-eastern Isuamiut. **C:** Climbing ripple marks in chloritic schist, south-western Qaqqarsuatsiaq. **D–E:** Chert and manganese-rich banded iron formation, northern Isuamiut. **F:** Climbing ripple marks in staurolite schist, north-eastern Equutiit Killiat. **G:** Andalusite-staurolite schist with repeated graded bedding and an upright fold, western Equutiit Killiat; arrows mark andalusite porphyroblasts up to 5 cm large in bedtops. **H:** Deformed mafic sill in andalusite-staurolite schist with contact aureole, western Equutiit Killiat. **J:** Finely laminated staurolite schist, north-eastern Equutiit Killiat. **K:** Intrusive contact between underside of sill and finely laminated staurolite schist with contact aureole, western Equutiit Killiat. Locations shown in Fig. 2.



Fig. 17. Relict Palaeoproterozoic dolerite dykes on island 11 km east of Aasiaat in the northern part of the Aasiaat domain (see Fig. 2). The intensely deformed dykes have been rotated into near-parallelism with their Archaean orthogneiss host during the Nagssugtoqidian orogeny. The dykes and their host rocks are cut by pink, late- to postkinematic Nagssugtoqidian pegmatites. From front cover of Garde & Kalsbeek (2006).

### Metadolerite (m)

Relict dolerite dykes of inferred Palaeoproterozoic age and presumably emplaced during pre-Nagssugtoqidian rifting are known from two parts of the map area.

Groups of E–W-trending, vertical, undeformed dolerite dykes with medium-grained amphibolite to granulite facies metamorphic textures occur in the southern part of the Aasiaat domain. Some of the dykes straddle the southern boundary of the map area at 68° latitude and have been described by Glassley & Sørensen (1980) and Árting (2004). The former authors studied the metamorphic evolution of the dykes. Árting (2004) observed planar and linear tectonic fabrics at the dyke margins and relict subophitic textures in their cores.

Being undeformed (unlike other relict dykes in the southern part of the map area) these dykes are of great interest as tectonic markers, because they show that the southern part of the Aasiaat domain acted as a stable block during the Nagssugtoqidian collision.

Intensely deformed and disrupted mafic dykes up to a couple of metres thick have been observed by boat in the archipelago north-east of Aasiaat (Fig. 17) and in Sydost-bugten east of the map area. These dykes have been

recrystallised into fine-grained amphibolite and commonly possess a strong schistosity and E–W-trending extension lineation of hornblende. They are flat-lying to moderately inclined, broadly conformable with their hosts of Archaean orthogneiss, and commonly display tectonic pinch-and-swell structure and boudinage, or are completely disrupted. A close inspection usually reveals a tight angular discordance between the dykes and their hosts. The dykes are in turn cut by undeformed Palaeoproterozoic pegmatites (Fig. 17). Such small pseudoconcordant dykes may also be common in inland areas but would be difficult to identify there, due to moss and lichen overgrowth.

### Granite and pegmatite (gp, P)

As mentioned in the general description of the Naternaq belt, irregular bodies of white, tourmaline-bearing pegmatite grading into coarse-grained, leucocratic, white to pink granite (gp) are commonly associated with the hinge zones of late folds in the belt. There are also isolated tourmaline-bearing pegmatites up to a few metres wide in areas where there are no folds (Fig. 15C).

Conjugate, late- to postkinematic pegmatites which are presumably related to N–S compression are also common (**P**, see Fig. 17). Thrane & Connelly (2006) obtained a  $^{207}\text{Pb}/^{206}\text{Pb}$  zircon age of  $1837 \pm 12$  Ma from a vertical pegmatite belonging to this group *c.* 25 km north-east of Kangaatsiaq, striking  $020^\circ$ . The dyke cuts

the ENE-trending Nagssugtoqidian foliation but its margins contain evidence of ductile sinistral shear. Its age is thus also the approximate minimum age of Nagssugtoqidian tectonic reworking in the northern part of the Asiaat domain.

## Cretaceous–Paleocene rocks

### Basalt, picritic (**b**)

Kitsissunnguit / Grønne Ejland in south-eastern Disko Bugt is a group of small islands which almost entirely consist of olivine basalt constituting a large dolerite sill. The sill at Grønne Ejland was emplaced into sediments close to the regional unconformity with the Precambrian basement. It has been dated at  $60.45 \pm 0.88$  Ma ( $^{40}\text{Ar}/^{39}\text{Ar}$  analysis on plagioclase, Larsen 2006) and was thus related to continental breakup and extrusion of the voluminous flood basalts in the Disko–Nuussuaq – Svartenhuk Halvø region. Another major sill complex in the Disko Bugt area, which includes exposures e.g. in Saqqaqdalen on Nuussuaq (Henderson *et al.* 1976), is of Early Eocene age (Storey *et al.* 1998).

### Sandstone (**st**)

A 4–6 m thick, non-marine section of cherty shale, chert, siltstone with plant remains and friable strongly convoluted sandstone, intercalated with tuffaceous material, forms a small occurrence on the south side of the south-easternmost island of Grønne Ejland in south-eastern Disko Bugt (Henderson *et al.* 1976). The presence of tuffaceous material indicates that the age of the sediments is Palaeogene. A sediment sample from Grønne Ejland was included in a survey of the detrital zircon age distribution in Cretaceous and Paleocene sandstones in West Greenland (Scherstén & Sønderholm 2007). The survey showed a Palaeoproterozoic peak and a larger composite Meso–Neoarchean peak all of which are probably locally sourced, as well as a few grains with Grenvillian ages which were interpreted as having a Canadian source.

### Dolerite dykes (**δ**)

Three major dykes are known to occur in the Asiaat region, one of which has been dated as Paleocene in age (see below). The dykes are plagioclase-clinopyroxene-olivine-phyric to aphyric and tholeiitic and have strongly chilled margins against their basement hosts (Larsen 2006). The dykes are clearly visible on the aeromagnetic maps of Fig. 4. The most studied dyke is the *c.* 60 km long, N–S-trending ‘globule dyke’ that occurs in the eastern part of the map area (Ellitsgaard-Rasmussen 1951; Árting 2004), and which has been dated at  $55.77 \pm 0.24$  Ma ( $^{40}\text{Ar}/^{39}\text{Ar}$  analysis on plagioclase, Larsen 2006). This dyke consists of globules or ellipsoids up to *c.* 20 cm in size with aphanitic mantles that are commonly surrounded by black volcanic glass. The globules are arranged in several adjacent ‘brick walls’ each about 1 m in thickness (Ellitsgaard-Rasmussen 1951). The peculiar structure of the dyke was most likely caused by contact with water during near-surface intrusion.

The two other dykes have homogeneous, medium-grained interiors. A 6–8 m thick, NNE-trending, side-stepping dyke occurs at Manermiut and can be followed as a strong linear feature with reversed magnetic polarity from 15 km south of Kangaatsiaq to well within Disko Bugt (Fig. 4). A second, 6–15 m thick, WNW-trending dyke occurs at Sydostbugten. This may be contiguous with an isolated dyke exposure near Asiaat.

## Quaternary deposits

The Quaternary deposits in the Kangaatsiaq and Ikamiut areas mainly consist of shallow marine silt that formed an outwash plain in front of the Akuliarutsip Sermersua / Nordenskiöld Gletscher east of the Kangaatsiaq map area and were subsequently raised above sea level during iso-

static rebound. Weidick & Bennike (2007) recently published an account of the Quaternary evolution in the adjacent Disko Bugt area, which also contains some general information about the Kangaatsiaq and Ikamiut areas.

## Archaean crustal evolution

### The Aasiaat domain: a distinct Archaean crustal segment

Most of the Aasiaat domain escaped intense reworking during the Nagssugtoqidian orogeny and therefore presents a window to study Archaean crustal evolution in central West Greenland. The idea that the northern part of the Nagssugtoqidian orogen is generally less intensely reworked than its central and southern parts is not new. For instance, Whitehouse *et al.* (1998) noted that two samples of Archaean biotite gneiss from the northern Nagssugtoqidian orogen did not show evidence of Palaeoproterozoic disturbance of their Rb-Sr isotopic systems, contrary to most samples of orthogneiss from the central part of the orogen. The same two samples have negative  $\epsilon_{\text{Nd}}(t)$  values of *c.* -2 and  $t_{\text{DM}}$  model ages 300–450 Ma in excess of their estimated emplacement ages, suggesting that these rocks contain evolved Nd from older crust.

The systematic new work for the two present map sheets produced much new evidence. Piazzolo *et al.* (2004), Mazur *et al.* (2006) and van Gool & Piazzolo (2006) demonstrated on structural grounds that a large part of the Aasiaat domain in the area between Kangaatsiaq and Nordre Strømfjord acted as a stable tectonic block during the Nagssugtoqidian orogeny, and the geotectonic significance of the metamorphosed but essentially undeformed, E-W-trending dykes near 68°N (which were originally described by Glassley & Sørensen 1980) was established. In addition, Connelly & Thrane (2005) showed that the Aasiaat domain has a different Pb-isotopic signature than the central and southern parts of the Nagssugtoqidian orogen although zircon ages obtained from orthogneisses in all these regions are similar, and suggested that the Archaean of the northern part of the Nagssugtoqidian orogen (*viz.* the Aasiaat domain) might represent a different segment of Archaean crust than the North Atlantic craton in the

south (Fig. 1). The Archaean age of the main phases of deformation, metamorphism and partial melting in the southern part of the Aasiaat domain was proven with the  $2748 \pm 19$  Ma age of a late-kinematic granite at Saqqarput obtained by Thrane & Connelly (2006).

### Archaean crustal accretion in arc environments, and evidence of Archaean rifting and sedimentation at the margins of the proto-Aasiaat domain

The main lithological components in the Aasiaat domain and their mutual relationships are broadly similar to those recently identified in six representative, upper to lower crustal blocks in the North Atlantic craton by Windley & Garde (2009) and interpreted as representing oceanic and continental arcs which eventually amalgamated into a continent.

As is evident from the map sheets and described by Hollis *et al.* (2006) and Moyén & Watt (2006) the supracrustal and associated rocks comprise tholeiites of volcanic and intrusive origin, smaller volumes of andesitic-dacitic and felsic volcanoclastic rocks of intermediate composition, gabbro-leucogabbro-anorthosite, as well as pelitic and not least quartzo-feldspathic sediment; the latter is relatively voluminous compared to most blocks in the North Atlantic craton. As shown by Hollis *et al.* (2006) and Moyén & Watt (2006), the Archaean orthogneisses within the map area are of TTG-type and were probably largely produced by slab melting. Minor dioritic components are also present, in which a mantle component has been identified (Steenfelt *et al.* 2005). Also late-kinematic crustal melt granites are present, like in most parts of the North Atlantic craton farther south.

The detrital rocks at Kangaatsiaq have chemical compositions corresponding to greywackes and shales and may have been sourced from both a mafic–intermediate arc and a gneissic basement (Moyen & Watt 2006). The Ikamiut belt contains detrital material that was at least in part sourced from, and deposited adjacent to the igneous precursors of Neoproterozoic granodioritic to tonalitic orthogneisses (Hollis *et al.* 2006). However, no depositional unconformity has so far been identified to underlie any of these sequences. Little detailed information exists about the quartzo-feldspathic rocks in the southern and south-eastern parts of the Kangaatsiaq map area. Where the nature of the original contacts has not been destroyed by deformation and metamorphism the TTG rocks generally have intrusive relationships with the supracrustal rocks. However, the contact relationships between the quartzo-feldspathic sedimentary units and adjacent orthogneiss are uncertain. Such uncertainty also remains at the previously mentioned locality on the south coast of Arfersiorfik close to the south-eastern corner of the Kangaatsiaq map area, where siliceous metasediment and marble occur at the base of a supracrustal sequence dominated by amphibolite. It may be significant that the *c.* 2850 Ma detrital zircon peak in quartz-rich metasediment at the head of Ataneq reported by Thrane & Connelly (2006) is compatible with derivation from the adjacent orthogneiss.

The Archaean tectono-metamorphic evolution in two small parts of the map area has been addressed by Hollis *et al.* (2006) and Moyen & Watt (2006), respectively. In both areas, early isoclinal folds have been refolded by one, two or three sets of overturned to upright folds. The deformation was accompanied by amphibolite facies and granulite facies metamorphism in the south. The ubiquitous presence of biotite and hornblende also in the granulite facies areas shows that the

granulite facies metamorphism was not accompanied by complete dehydration and was most likely of the thermal type described by Wells (1980), which is characteristic of large parts of the North Atlantic craton.

Detailed analysis of the Archaean geotectonic evolution is not attempted here. However, it may be noted that the tholeiitic and intermediate metavolcanic rocks are largely concentrated in a few moderately to steeply inclined belts up to *c.* 2 km thick with an overall NE–SW trend. In contrast the quartzo-feldspathic paragneisses are largely concentrated in the Kangaatsiaq, Amitsoq and Ikamiut areas in the vicinity of the present northern and southern margins of the Aasiaat domain. This distribution might suggest that the magmatic and tectonic accretion of the Aasiaat domain took place in two main stages separated by rifting and sedimentation. In the first stage, several arc systems, which are now represented by TTG plutons enveloped by large amphibolite belts, were amalgamated into a proto-Aasiaat domain. Then followed rifting and injection of mafic dykes, which can still be identified as widespread, deformed dyke fragments within the southern part of the Aasiaat domain that was not reworked in the Palaeoproterozoic (see Fig. 7). No age data are available from the paragneiss at Kangaatsiaq, but intrusive orthogneiss contacts have not been documented. It has previously been shown that the quartzo-feldspathic paragneisses in Ikamiut area are younger than the adjacent TTG-type orthogneisses (Hollis *et al.* 2006), and the same may well be the case for the paragneiss at Amitsoq in view of the 2850 Ma detrital zircon peak reported by Thrane & Connelly (2006). Also the latter metasedimentary rocks may well represent younger continental margin sediment that was deposited on the outboard sides of the proto-Aasiaat domain, and which were in turn deformed and metamorphosed during a second Archaean orogenic phase.

## Palaeoproterozoic tectonic evolution and plate-tectonic model

The Palaeoproterozoic evolution of West Greenland in a plate-tectonic context has been addressed in several publications over the last decade as summarised in the introduction. Garde & Hollis (2010) recently presented a different plate-tectonic interpretation of the Nagssugtoqidian orogen, which is briefly outlined in the following. Their model is based on the recognition of the stable Aasiaat domain, and of a Palaeoproterozoic ocean floor –

arc trench assemblage and a buried spreading ridge on islands north-east of Aasiaat. These observations require a suture to be present between the islands and the reworked Archaean rocks of the Aasiaat domain to the south of the islands, and thus necessitate a revision of the previous plate-tectonic model for the Nagssugtoqidian orogen (van Gool *et al.* 2002; van Gool & Marker 2007). The insight that the Nagssugtoqidian orogen and Rink-

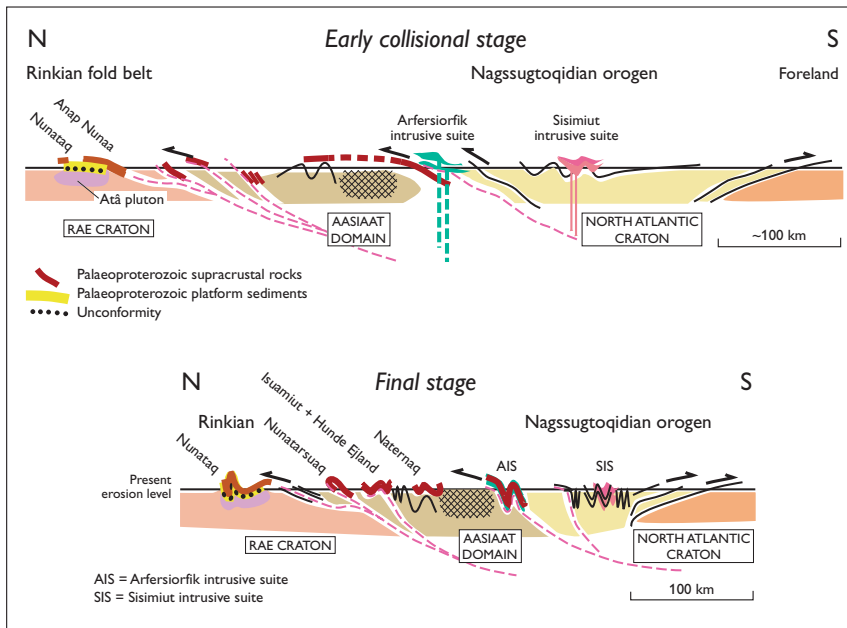


Fig. 18. Plate-tectonic model for the Nagssugtoqidian orogen from north to south along the length of the map in Fig. 1, from Garde & Hollis (2010). The new model has two SSE-dipping sutures (viz. subduction zones), each of which can be correlated with a Palaeoproterozoic magmatic arc. The northern subduction zone (Disko Bugt suture) fed the oceanic Arfersiorfik intrusive complex south of the Aasiaat domain, whereas the previously established southern subduction zone (central Nagssugtoqidian suture) fed the continental Sisimiut intrusive suite that was emplaced into the North Atlantic craton. See the main text for discussion of the individual supracrustal and intrusive units.

ian fold belt represent the southern and northern parts of one major collisional orogenic system between the Rae and North Atlantic cratons in western Greenland and eastern Canada, and the proposal of a suture zone at Paakitsoq in the southern Rinkian fold belt by Connelly *et al.* (2006) were major first steps in this revision.

The new plate-tectonic model for the Nagssugtoqidian orogen and the southern part of the Rinkian fold belt is shown in Fig. 18. It was initially presented as a rough idea by Garde *et al.* (2007a) and was subsequently incorporated into the correlation between the Palaeoproterozoic in eastern Canada and western Greenland by St-Onge *et al.* (2009), where the Aasiaat domain and new Disko Bugt suture were first labelled. In the new model

there are two S- to SE-dipping subduction zones in the central and northern Nagssugtoqidian orogen, respectively, which are separated by the Aasiaat domain. The new suture on the north side of the Aasiaat domain can be linked with the proposed suture at Paakitsoq by Connelly *et al.* (2006) that appears to form a tectonic splay system in the Ilulissat area separating the Rae craton and the Aasiaat domain (Figs 1, 18). A continuation of this splay system is proposed to exist north of Aasiaat as indicated on Fig. 1 (see also Garde & Hollis 2010).

In the new model the 1895 Ma Arfersiorfik intrusive suite (Fig. 18) is interpreted to have been fed by the northernmost of the two subduction zones. The Arfersiorfik intrusive suite itself presumably represents the



Fig. 19. N-directed, stacked thrust sheets of Archaean orthogneiss and brown, rusty-weathering Palaeoproterozoic supracrustal rocks (arrow) at the southern margin of the Aasiaat domain. View from helicopter towards the east at the head of Ataneq, just south of the Kangaatsiaq map area.

plutonic root system of an arc that was located in the ocean which separated the Aasiaat domain from the North Atlantic craton prior to the Nagssugtoqidian collision. The suture in the central Nagssugtoqidian orogen that was proposed in the original plate-tectonic model, is located between the Aasiaat domain and the North Atlantic craton. According to the new model the corresponding subduction system only fed the Sisimiut intrusive suite. This suite was emplaced within the North Atlantic craton that formed the southern collisional continent, and is thus a continental arc.

The Naternaq supracrustal belt is interpreted on Fig. 18 as having been extruded by tectonic forces from the southern collision zone along a major N-directed thrust system which transported it to its present, discordant position on top of the Aasiaat domain. The photograph of Fig. 19 shows a stack of such northward-directed thrust sheets at the southern margin of the Aasiaat domain. Unfortunately the Naternaq supracrustal belt is at a relatively high metamorphic grade and mostly very intensely deformed, and this hinders proper identifica-

tion of its volcanic and sedimentary precursors. Further work is thus required to resolve if its fine-grained amphibolites represent ocean floor volcanics or were generated in an arc or supra-subduction zone.

The northern part of the schematic cross-section of Fig. 18 includes three other localities north of the Ikamiut map area that belong to the Rinkian fold belt. (1) The isoclinally folded, fine-grained amphibolite and mica schist at Nunatarsuaq are of Palaeoproterozoic age (Connelly *et al.* 2006), and these poorly preserved rocks may be broadly equivalent to those occurring at the Isuamiut–Qaqqarsuatsiaq – Equutiit Killiat islands. (2) The Anap nunâ Group farther north at Anap Nunaa and (3) the Palaeoproterozoic component of Nunataq (Figs 1, 18) consist of platform sediments which were deposited at the southern, passive margin of the Rae craton, and a basal unconformity is preserved (Garde & Steenfelt 1999; Higgins & Soper 1999). Furthermore, the Anap nunâ Group is correlated with the Karrat Group in the core of the Rinkian fold belt (Henderson & Pulvertaft 1987; St-Onge *et al.* 2009).

## Economic geology

An overview of all known mineral occurrences in central West Greenland from 66° N to 70°15' N can be found in Survey reports by Schjøth & Steenfelt (2004) and Stendal *et al.* (2004). The Archaean base metal occurrences that have been identified to date are insignificant both in terms of their frequency and size and will not be discussed further here. There are no known occurrences of gold or platinum group elements in the map sheet area, but there may be a gold potential in Archaean amphibolites, especially since some of them e.g. east of Kangaatsiaq have been shown to be arc-related. The potential for dimension stone has not been evaluated but is not considered very promising due to strong Palaeoproterozoic tectonic reworking in part of the map area, and the heterogeneous nature of the basement rocks in the southern Aasiaat domain. However, the granodiorites and granites on Maniitsoq and Kronprinsens Ejland in the north might possess a potential.

From an economic point of view the most important occurrences in the map area are probably volcanic-hosted massive sulphide (VHMS-type) deposits of Palaeoproterozoic age. Semi-massive to massive, pyrrhotite-rich sulphide mineralised zones are located in the Naternaq supracrustal belt. The largest mineralised zones just east

of the Kangaatsiaq map boundary were discovered and investigated by Kryolitselskabet Øresund A/S in the 1960s, and were described by Østergaard *et al.* (2002). Massive VHMS-type rocks typically form up to *c.* 2 m wide and 4 m long lenses (maximum size 2 × 10 m); the mineralised rocks are iron-rich and dominated by pyrrhotite, with minor chalcopyrite and sphalerite (up to *c.* 3%) and subordinate pyrite, arsenopyrite, magnetite and graphite. Thinner, conformable horizons containing disseminated to semi-massive sulphides may be followed for up to a few hundred metres. Information about the host rocks can be found in the descriptions of marble and calc-silicate rocks (c) and volcanogenic-exhalative horizons with chert and sulphidic rocks (v), and in Østergaard *et al.* (2002).

Another sulphide occurrence was reported by an inhabitant of Hunde Ejland *c.* 15 km north-northwest of Aasiaat in the 2004 'Ujarassiorit' campaign organised by the Greenland Home Rule Government. As stated in a previous section this island group consists of amphibolite facies, low-strain, very fine-grained volcanic and hypabyssal mafic rocks as well as aluminous and siliceous clastic rocks which resemble the ocean floor – arc trench rock associations found on the Isuamiut–Qaqqarsuatsiaq

– Equutiit Killiat islands. Accordingly, the rocks on Hunde Ejlande are likely to be of Palaeoproterozoic age. Several sulphidic, iron-rich quartz vein samples with VHMS-style Cu-Zn-Au-Ag-Hg-Se mineralisation occur, and a chemical analysis of one of them is reproduced in Garde & Hollis (2010); such VHMS-type mineralisation may be found today in 'black smokers' on the ocean floor. More work on Hunde Ejlande is required to substantiate the age, setting and significance of its host rocks and mineralisation.

Palaeoproterozoic banded iron formation occurs both on the islands of Isuamiut and Qaqqarsuatsiaq where it is in oxide facies and contains around 3 wt% MnO, and in the Naternaq supracrustal belt where it is in carbonate facies (Fig. 15B; Østergaard *et al.* 2002). The occurrence described in the latter publication is located just east of the map boundary, but there may be others inside it. None of these deposits are sufficiently large to be considered of economic interest.

## Acknowledgements

The contributions by the geologists listed on the index maps of the two map sheets in the form of field maps, reports and publications also form an indispensable basis for the present work. Annette Thorning Hindø, Hans Jepsen, Jørgen Neve and Willy Weng carried out the digital production of the map sheets and kindly provided support for photogrammetrical interpretation. Stanislaw Mazur and Claus Østergaard are thanked for unravelling complicated rock exposures and structures in parts of the Naternaq supracrustal belt, although the responsibility for the possibly erroneous overall interpretation rests with the authors. We also thank M. Whitehouse and L. Ilievsky at the ion microprobe laboratory in Stockholm (NORDSIM) for help with acquisition and handling of the geochronological data. The laboratory is operated by agreement between the joint Nordic research councils (NOS-N), the Geological Survey of Finland, and the Swedish Museum of Natural History. Thorkild M. Rasmussen supplied Fig. 4 and helped with interpretation of the aeromagnetic data. The authors are grateful to Sandra Piazzolo for reviewing the manuscript.

## References

- Árting, U.E. 2004: A petrological study of basic dykes and sills of assumed Palaeoproterozoic age in central West Greenland, 121 pp. + appendices. Unpublished MSc thesis, University of Copenhagen, Denmark.
- Connelly, J.N. & Thrane, K. 2005: Rapid determination of Pb isotopes to define Precambrian allochthonous domains: an example from West Greenland. *Geology* **33**, 953–956.
- Connelly, J.N., van Gool, J.A.M. & Mengel, F.C. 2000: Temporal evolution of a deeply eroded orogen: the Nagssugtoqidian orogen, West Greenland. *Canadian Journal of Earth Sciences* **37**, 1121–1142.
- Connelly, J.N., Thrane, K., Krawiec, A.W. & Garde, A.A. 2006: Linking the Palaeoproterozoic Nagssugtoqidian and Rinkian orogens through the Disko Bugt region of West Greenland. *Journal of the Geological Society (London)* **163**, 319–335.
- Ellitsgaard-Rasmussen, K. 1951: A West Greenland globule dike. *Meddelelser fra Dansk Geologisk Forening* **12**, 83–101.
- Ellitsgaard-Rasmussen, K. 1954: On the geology of a metamorphic complex in West Greenland. The islands of Anarssuit, Isuamiut, and Equitit. *Bulletin Grønlands Geologiske Undersøgelse* **5**, 70 pp.
- Escher, A. 1971: Geological map of Greenland, 1:500 000, Søndre Strømfjord – Nûgssuaq, Sheet 3. Copenhagen: Geological Survey of Greenland.
- Escher, A., Sørensen, K. & Zeck, H.P. 1976: Nagssugtoqidian mobile belt in West Greenland. In: Escher, A. & Watt, W.S. (eds): *Geology of Greenland*, 105–119. Copenhagen: Geological Survey of Greenland.
- Garde, A.A. 2004: Geological map of Greenland, 1:100 000, Kangaatsiaq 68 V.1 Syd. Copenhagen: Geological Survey of Denmark and Greenland.
- Garde, A.A. 2006: Geological map of Greenland, 1:100 000, Ikamiut 68 V.1 Nord. Copenhagen: Geological Survey of Denmark and Greenland.
- Garde, A.A. 2008: Geochemistry of Mesoarchean andesitic rocks with epithermal gold mineralisation at Qussuk and Bjørneøen, southern West Greenland. *Danmarks og Grønlands Geologiske Undersøgelse Rapport* **2008/4**, 52 pp.
- Garde, A.A. & Hollis, J.A. 2010: A buried Palaeoproterozoic spreading ridge in the northern Nagssugtoqidian orogen, West Greenland. In: Kusky, T.M., Zhai, M.-G. & Xiao, W. (eds): *The evolving continents: understanding processes of continental growth*. Geological Society Special Publication (London) **338**, 213–234.
- Garde, A.A. & Kalsbeek, F. (eds) 2006: Precambrian crustal evolution and Cretaceous–Palaeogene faulting in West Greenland. *Geological Survey of Denmark and Greenland Bulletin* **11**, 204 pp.
- Garde, A.A. & Steenfelt, A. 1999: Precambrian geology of Nuussuaq and the area north-east of Disko Bugt, West Greenland. In: Kalsbeek, F. (ed.): *Precambrian geology of the Disko Bugt region, West Greenland*. *Geology of Greenland Survey Bulletin* **181**, 7–40.

- Garde, A.A., Grocott, J., Thrane, K. & Connelly, J.N. 2003: Reappraisal of the Rinkian fold belt in central West Greenland: tectonic evolution during crustal shortening and linkage with the Nagssugtoqidian orogen. *Geophysical Research Abstracts* **5** (EGS-AGU-EUG Joint Assembly), 09411 only.
- Garde, A.A., Christiansen, M.J., Hollis, J.A., Mazur, S. & van Gool, J.A.M. 2004: Low-pressure metamorphism during Archaean crustal growth: a low-strain zone in the northern Nagssugtoqidian orogen, West Greenland. *Geological Survey of Denmark and Greenland Bulletin* **4**, 73–76.
- Garde, A.A., Hollis, J.A. & Mazur, S. 2007a: Palaeoproterozoic greenstones and pelitic schists in the northern Nagssugtoqidian orogen, West Greenland: evidence for a second subduction zone? Geological Association of Canada – Mineralogical Association of Canada (GAC-MAC) annual meeting, Yellowknife 2007, Program with Abstracts.
- Garde, A.A., Stendal, H. & Stensgaard, B.M. 2007b: Pre-metamorphic hydrothermal alteration with gold in a mid-Archaean island arc, Godthåbsfjord, West Greenland. *Geological Survey of Denmark and Greenland Bulletin* **13**, 37–40.
- Glassley, W.E. & Sørensen, K. 1980: Constant P<sub>s</sub>-T amphibolite to granulite facies transition in Agto (West Greenland) metadolerites: implications and applications. *Journal of Petrology* **21**, 69–105.
- Henderson, G. 1969: The Precambrian rocks of the Egedesminde-Christianshåb area, West Greenland. *Rapport Grønlands Geologiske Undersøgelse* **23**, 37 pp.
- Henderson, G. & Pulvertaft, T.C.R. 1987: Geological map of Greenland, 1:100 000, Marmorilik 71 V.2 Syd, Nûgâtsiaq 71 V.2 Nord, Pangnertôq 72 V.2 Syd. Descriptive text, 72 pp., 8 plates. Copenhagen: Grønlands Geologiske Undersøgelse [Geological Survey of Greenland].
- Henderson, G., Rosenkrantz, A. & Schiener, E.J. 1976: Cretaceous–Tertiary sedimentary rocks of West Greenland. In: Escher, A. & Watt, W.S. (eds): *Geology of Greenland*, 340–362. Copenhagen: Geological Survey of Greenland.
- Higgins, A.K. & Soper, N.J. 1999: The Precambrian supracrustal rocks of Nunataq, north-east Disko Bugt, West Greenland. In: Kalsbeek, F. (ed.): *Precambrian geology of the Disko Bugt region, West Greenland*. *Geology of Greenland Survey Bulletin* **181**, 79–86.
- Hollis, J.A., Keiding, M., Stensgaard, B.M., van Gool, J.A.M. & Garde, A.A. 2006: Evolution of Neoproterozoic supracrustal belts at the northern margin of the North Atlantic craton, West Greenland. In: Garde, A.A. & Kalsbeek, F. (eds): *Precambrian crustal evolution and Cretaceous–Palaeogene faulting in West Greenland*. *Geological Survey of Denmark and Greenland Bulletin* **11**, 9–31.
- Kalsbeek, F. & Nutman, A.P. 1996: Anatomy of the Early Proterozoic Nagssugtoqidian orogen, West Greenland, explored by reconnaissance SHRIMP U-Pb dating. *Geology* **24**, 515–518.
- Kalsbeek, F. & Taylor, P.N. 1999: Review of isotope data for Precambrian rocks from the Disko Bugt region, West Greenland. In: Kalsbeek, F. (ed.): *Precambrian geology of the Disko Bugt region, West Greenland*. *Geology of Greenland Survey Bulletin* **181**, 41–47.
- Kalsbeek, F., Bridgwater, D. & Zeck, H.P. 1978: A  $1950 \pm 60$  Ma Rb-Sr whole-rock isochron age from two Kangâmiut dykes and the timing of the Nagssugtoqidian (Hudsonian) orogeny in West Greenland. *Canadian Journal of Earth Sciences* **15**, 1122–1128.
- Kalsbeek, F., Taylor, P.N. & Henriksen, N. 1984: Age of rocks, structures and metamorphism in the Nagssugtoqidian mobile belt, West Greenland – field and Pb isotope evidence. *Canadian Journal of Earth Sciences* **21**, 1126–1131.
- Kalsbeek, F., Pidgeon, R.T. & Taylor, P.N. 1987: Nagssugtoqidian mobile belt of West Greenland: a cryptic 1850 Ma suture between two Archaean continents – chemical and isotopic evidence. *Earth and Planetary Science Letters* **85**, 365–385.
- Korstgård, J.A. (ed.) 1979: Nagssugtoqidian geology. *Rapport Grønlands Geologiske Undersøgelse* **89**, 146 pp.
- Kystøl, J. & Larsen, L.M. 1999: Analytical procedures in the Rock Geochemical Laboratory of the Geological Survey of Denmark and Greenland. *Geology of Greenland Survey Bulletin* **184**, 59–62.
- Larsen, L.M. 2006: Mesozoic to Palaeogene dyke swarms in West Greenland and their significance for the formation of the Labrador Sea and the Davis Strait. *Danmarks og Grønlands Geologiske Undersøgelse Rapport* **2006/34**, 69 pp. + 2 appendices.
- Ludwig, K.R. 2000: *Isoplot/Ex version 2.2: a geochronological toolkit for Microsoft Excel*. Berkeley: Berkeley Geochronological Center.
- Mazur, S., Piazzolo, S. & Alsop, G.I. 2006: Structural analysis of the northern Nagssugtoqidian orogen, West Greenland: an example of complex tectonic patterns in reworked high-grade metamorphic terrains. In: Garde, A.A. & Kalsbeek, F. (eds): *Precambrian crustal evolution and Cretaceous–Palaeogene faulting in West Greenland*. *Geological Survey of Denmark and Greenland Bulletin* **11**, 163–178.
- Moyen, J.-F. & Watt, G.R. 2006: Pre-Nagssugtoqidian crustal evolution in West Greenland: geology, geochemistry and deformation of supracrustal and granitic rocks north-east of Kangaatsiaq. In: Garde, A.A. & Kalsbeek, F. (eds): *Precambrian crustal evolution and Cretaceous–Palaeogene faulting in West Greenland*. *Geological Survey of Denmark and Greenland Bulletin* **11**, 33–52.
- Myers, J.S. 1985: Stratigraphy and structure of the Fiskensætt Complex, southern West Greenland. *Bulletin Grønlands Geologiske Undersøgelse* **150**, 72 pp.
- Nielsen, B.M. & Rasmussen, T.M. 2004: Mineral resources of the Precambrian shield of central West Greenland (66° to 70°15'N). Part 3. Implications of potential field data for the tectonic framework. *Danmarks og Grønlands Geologiske Undersøgelse Rapport* **2004/21**, 165 pp.
- Noe-Nygaard, A. & Ramberg, H. 1961: Geological reconnaissance map of the country between latitudes 69°N and 63°45'N, West Greenland. *Meddelelser om Grønland* **123**(5), 9 pp.
- Olesen, N.Ø. 1984: Geological map of Greenland, 1:100 000, Agto 67 V.1 Nord. Copenhagen: Geological Survey of Greenland.
- Østergaard, C., Garde, A.A., Nygaard, J., Blomsterberg, J., Nielsen, B.M., Stendal, H. & Thomas, C.W. 2002: The Precambrian supracrustal rocks in the Naternaq (Lersletten) and Ikamiut areas, central West Greenland. *Geology of Greenland Survey Bulletin* **191**, 24–32.
- Piazzolo, S., Alsop, G.I., van Gool, J. & Nielsen, B.M. 2004: Using GIS to unravel high strain patterns in high grade terranes: a case study of indentor tectonics from West Greenland. In: Alsop, G.I. *et al.* (eds): *Flow processes in faults and shear zones*. *Geological Society Special Publications* (London) **224**, 63–78.

- Ramberg, H. 1949: On the petrogenesis of the gneiss complexes between Sukkertoppen and Christianshaab, West Greenland. *Meddelelser fra Dansk Geologisk Forening* **11**, 312–327.
- Rasmussen, T.M. & van Gool, J.A.M. 2000: Aeromagnetic survey in southern West Greenland: project Aeromag 1999. *Geology of Greenland Survey Bulletin* **186**, 73–77.
- Scherstén, A. & Sønderholm, M. 2007: Provenance of Cretaceous and Paleocene sandstones in the West Greenland basins based on detrital zircon dating. *Geological Survey of Denmark and Greenland Bulletin* **13**, 29–32.
- Schjøth, F. & Steenfelt, A. 2004: Mineral resources of the Precambrian shield of central West Greenland (66° to 70°15'N). Part 1. Compilation of geoscience data. *Danmarks og Grønlands Geologiske Undersøgelse Rapport 2004/16*, 45 pp., 1 DVD.
- Sidgren, A.-S., Page, L. & Garde, A.A. 2006: New hornblende and muscovite  $^{40}\text{Ar}/^{39}\text{Ar}$  cooling ages in the central and northern Nagssugtoqidian orogen, West Greenland. In: Garde, A.A. & Kalsbeek, F. (eds): *Precambrian crustal evolution and Cretaceous–Palaeogene faulting in West Greenland*. Geological Survey of Denmark and Greenland Bulletin **11**, 115–123.
- Steenfelt, A., Garde, A.A. & Moyon, J.-F. 2005: Mantle wedge involvement in the petrogenesis of Archaean grey gneisses in West Greenland. *Lithos* **79**, 207–228.
- Stendal, H., Nielsen, B.M., Secher, K. & Steenfelt, A. 2004: Mineral resources of the Precambrian shield of central West Greenland (66° to 70°15'N). Part 2. Mineral occurrences. *Danmarks og Grønlands Geologiske Undersøgelse Rapport 2004/20*, 212 pp.
- St-Onge, M., van Gool, J.A.M., Garde, A.A. & Scott, D.J. 2009: Correlation of Archaean and Palaeoproterozoic units between northeastern Canada and western Greenland: constraining the pre-collisional upper plate accretionary history of the Trans-Hudson orogen. In: Cawood, P.A. & Kröner, A. (eds): *Earth accretionary systems in space and time*. Geological Society Special Publications (London) **318**, 193–235.
- Storey, M., Duncan, R.A., Pedersen, A.K., Larsen, L.M. & Larsen, H.C. 1998:  $^{40}\text{Ar}/^{39}\text{Ar}$  geochronology of the West Greenland Tertiary volcanic province. *Earth and Planetary Science Letters* **160**, 569–586.
- Thorning, L. 1993: Project AEROMAG-92: a new high resolution aeromagnetic survey of the Lersletten area, central West Greenland (68°15' to 68°55'N, 50°25' to 53°35'W). *Open File Series Grønlands Geologiske Undersøgelse* **93/2**, 34 pp.
- Thrane, K. & Connelly, J.N. 2006: Zircon geochronology from the Kangaatsiaq–Qasigianniguit region, the northern part of the 1.9–1.8 Ga Nagssugtoqidian orogen, West Greenland. In: Garde, A.A. & Kalsbeek, F. (eds): *Precambrian crustal evolution and Cretaceous–Palaeogene faulting in West Greenland*. Geological Survey of Denmark and Greenland Bulletin **11**, 7–40.
- Thrane, K., Connelly, J.N., Garde, A.A., Grocott, J. & Krawiec, A.W. 2003: Linking the Palaeoproterozoic Rinkian and Nagssugtoqidian belts of central West Greenland: implications of new U-Pb and Pb-Pb zircon ages. *Geophysical Research Abstracts* **5** (EGS-AGU-EUG Joint Assembly), 09275 only.
- van Gool, J.A.M. 2005: Geological map of Greenland, 1:100 000, Kangersuneq 68 V.2 Nord. Copenhagen: Geological Survey of Denmark and Greenland.
- van Gool, J.A.M. & Marker, M. 2004: Geological map of Greenland, 1:100 000, Ussuit 67 V.2 Nord. Copenhagen: Geological Survey of Denmark and Greenland.
- van Gool, J.A.M. & Marker, M. 2007: Explanatory notes to the Geological map of Greenland, 1:100 000, Ussuit 67 V.2 Nord. Geological Survey of Denmark and Greenland Map Series **3**, 40 pp. + map.
- van Gool, J.A.M. & Piaolo, S. 2006: Presentation and interpretation of structural data from the Nagssugtoqidian orogen using a GIS platform: general trends and features. In: Garde, A.A. & Kalsbeek, F. (eds): *Precambrian crustal evolution and Cretaceous–Palaeogene faulting in West Greenland*. Geological Survey of Denmark and Greenland Bulletin **11**, 125–144.
- van Gool, J.A.M., Connelly, J.N., Marker, M. & Mengel, F.C. 2002: The Nagssugtoqidian Orogen of West Greenland: tectonic evolution and regional correlations from a West Greenland perspective. *Canadian Journal of Earth Sciences* **39**, 665–686.
- Weidick, A. & Bennike, O. 2007: Quaternary glaciation history and glaciology of Jakobshavn Isbræ and the Disko Bugt region, West Greenland: a review. *Geological Survey of Denmark and Greenland Bulletin* **14**, 78 pp.
- Wells, P.R.A. 1980: Thermal models for the magmatic accretion and subsequent metamorphism of continental crust. *Earth and Planetary Science Letters* **46**, 253–265.
- Whitehouse, M.J., Claesson, S., Sunde, T. & Vestin, J. 1997: Ion microprobe U-Pb zircon geochronology and correlation of Archaean gneisses from the Lewisian Complex of Gruinard Bay, northwestern Scotland. *Geochimica et Cosmochimica Acta* **61/20**, 4429–4438.
- Whitehouse, M.J., Kalsbeek, F. & Nutman, A.P. 1998: Crustal growth and crustal recycling in the Nagssugtoqidian orogen of West Greenland: constraints from radiogenic isotope systematics and U-Pb zircon geochronology. *Precambrian Research* **91**, 365–381.
- Whitehouse, M.J., Kamber, B.S. & Moorbath, S. 1999: Age significance of U-Th-Pb zircon data from early Archaean rocks of West Greenland – a reassessment based on combined ion-microprobe and imaging studies. *Chemical Geology* **160**, 201–224.
- Wiedenbeck, M., Alle, P., Corfu, F., Griffin, W.L., Meier, M., Oberli, F., von Quadt, A., Roddick, J.C. & Spiegel, W. 1995: Three natural zircon standards for U-Th-Pb, Lu-Hf, trace element and REE analyses. *Geostandards Newsletter* **19/1**, 1–23.
- Windley, B.F. & Garde, A.A. 2009: Arc-generated blocks with crustal sections in the North Atlantic craton of West Greenland: crustal growth in the Archean with modern analogues. *Earth-Science Reviews* **93**, 1–30.

# Appendix: zircon U-Pb geochronological data

## Sample preparation and analytical methods

The three samples described in the following were crushed, sieved and their zircons separated at the Geological Survey of Denmark and Greenland as described by van Gool & Marker (2007). The grains were mounted together with reference zircon 91500 (Ontario, Canada, weighted average  $^{207}\text{Pb}/^{206}\text{Pb}$  age of 1065 Ma, Wiedenbeck *et al.* 1995). Zircon morphologies were identified using backscattered electron imaging using a Philips XL 40 scanning electron microscope at GEUS, operating at 20kV and a working distance of 10 mm. U-Pb zircon data were collected using a Cameca IMS 1270 secondary ion mass spectrometer at the NORDSIM laboratory, Swedish Museum of Natural History, Stockholm. Analytical procedures and common lead corrections are similar to those described by Whitehouse *et al.* (1997, 1999). U-Pb concordia ages were calculated using IsoPlot (Ludwig 2000).

## Orthogneiss 467558, island east of Maniitsoq

A weakly deformed, medium-grained, grey orthogneiss with intrusive contacts into supracrustal amphibolite was sampled on the west coast of a small elongate island just east of Maniitsoq (Fig. 2). A photograph of the sample-

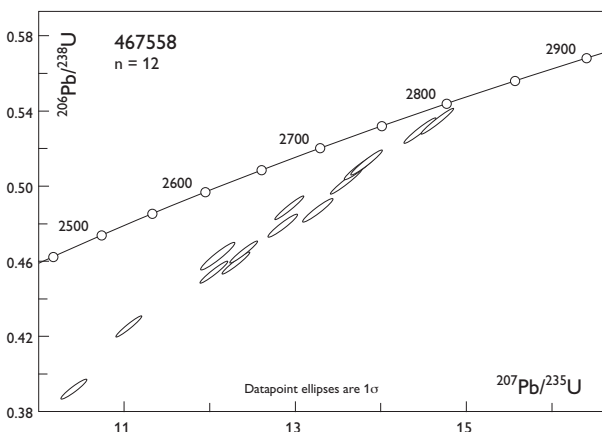


Fig. 20. U-Pb concordia diagram for sample 467558, a  $\geq 2810$  Ma Archaean orthogneiss with intrusive contact to supracrustal rocks on island east of Maniitsoq. Only an approximate age of 2810 Ma (or older) could be obtained due to scatter of the datapoints beyond the analytical precision, which may be due to early lead loss. Sample location given in Table 1.

locality was published by Garde *et al.* (2004), who thought that the supracrustal rocks intruded by the orthogneiss precursor represented a lateral continuation of the lower-grade greenstones on the Isuamiut–Qaqqarsuatsiaq islands (now known to be of Palaeoproterozoic age; Garde & Hollis 2010). The location and major and trace element compositions of this sample are given in Table 1, and the geochronological data in Fig. 20 and Table 3.

The zircon grains are elongate, typically about 200  $\mu\text{m}$  long, and display oscillatory zonation typically found in igneous zircon, and no distinct metamorphic rims were observed. No isochron or valid Pb-Pb age could be calculated, as a whole range of ages between *c.* 2815 and 2750 Ma were obtained from individual grains (see Fig. 20 and

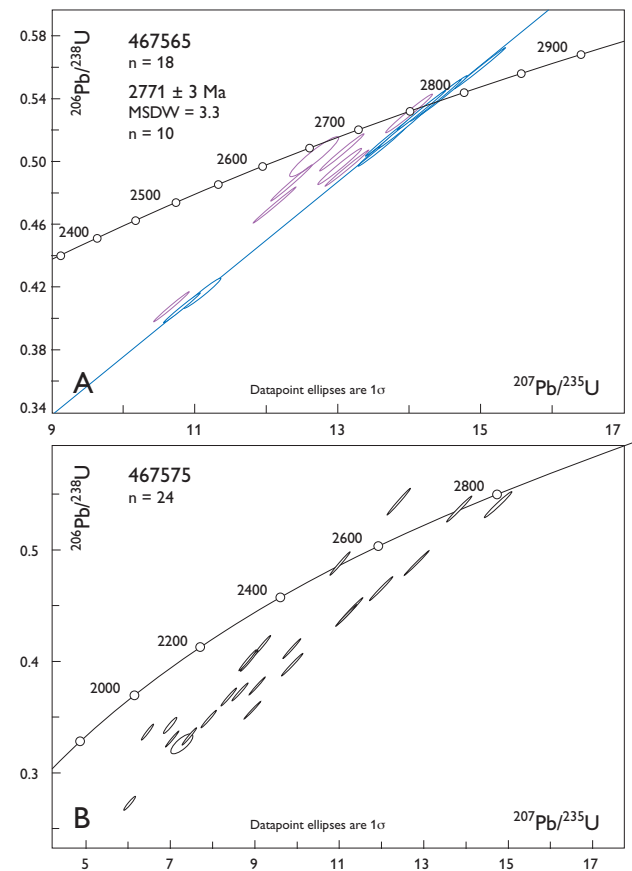


Fig. 21. U-Pb concordia diagrams for two samples of Neoproterozoic granodiorite at Maniitsoq and adjacent islands north of Aasiaat. The grains with the oldest ages in sample 467565 (Fig. 21A) yield an isochron with an age of  $2771 \pm 3$  Ma, which is geologically meaningful. The large scatter of datapoints, especially in sample 467575, is interpreted as due to early lead loss in the relatively U- and Th-rich zircon crystals.

Table 3). The oldest grains indicate an emplacement age of at least *c.* 2810 Ma. The lower Pb-Pb ages of many grains suggest they have been variably and commonly significantly affected by early lead loss.

### **K-feldspar porphyritic granodiorite 467565, Maniitsoq and 467575, adjacent island**

Geochronological data were obtained from two samples of the homogeneous, weakly deformed, medium-grained, K-feldspar megacrystic granodiorite that crops out on Maniitsoq and adjacent islands (Fig. 2), and which in several places contains magmatic enclaves of various sillimanite-grade metasedimentary rocks and supracrustal amphibolite.

Major and trace element analysis and sample coordinates are given in Table 1, and zircon U-Pb ion microprobe geochronology in Table 3 and Fig. 21. Sample 467565, collected on the triangular island south-west of Maniitsoq (Fig. 2), yielded an age of  $2771 \pm 3$  Ma (MSWD = 3.3) based on the ten oldest of 18 analysed grains (Table 3, Fig. 21A). The zircon crystals in these samples are stubby to elongate prisms that are typically around 200–300  $\mu\text{m}$  long. On scanning electron microscope backscatter images the zircon crystals display very conspicuous oscillatory zoning and occasional homogeneous rims of likely metamorphic origin that are too narrow to be analysed (Fig. 22).

The second sample of granodiorite (467575) was collected on the south coast of Maniitsoq island. The zircon morphology is the same as already described for sample 467565, and the geochronological data are likewise of good analytical quality. Twenty-one analytical spots in 18 grains were analysed. The ages of individual zircon crystals fall in a wide range between *c.* 2600 and 2800 Ma (Fig. 21B), and the oldest, low-U and low-Th grains point to a minimum age of emplacement of about 2750 Ma. Within error this age is consistent with the age of

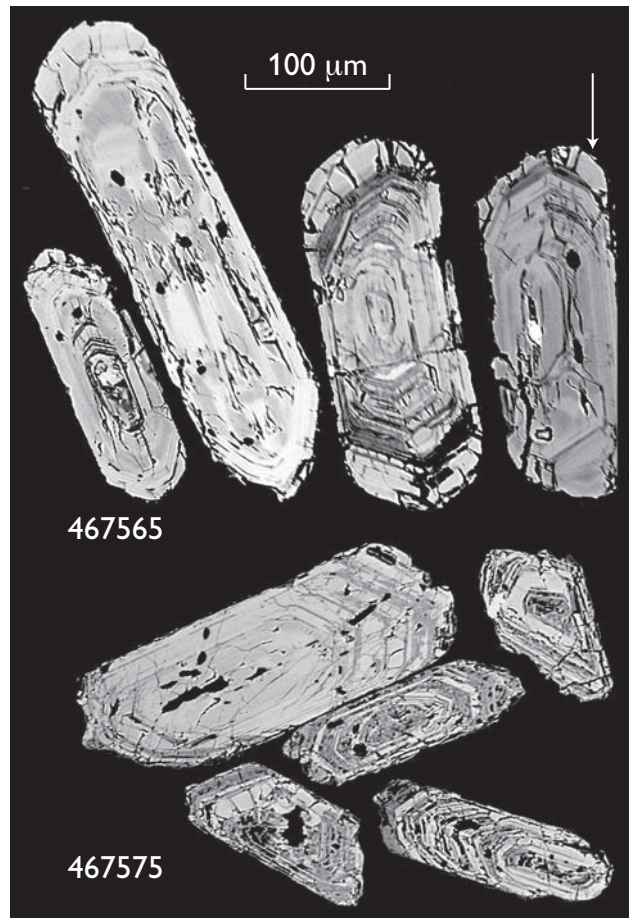


Fig. 22. Backscatter electron images of zircon grains in samples 467565 and 467575 displaying strong igneous-type, oscillatory zonation and many cracks. Narrow metamorphic overgrowths that could not be analysed are observed in sample 467565 (arrow).

$2771 \pm 3$  Ma obtained from sample 467565. Numerous other grains yield younger apparent ages. These grains are U- and Th-rich (typically with around 1000 ppm U and 500 ppm Th; Table 3), and are considered likely to have undergone substantial early lead loss, like in the nearby sample of tonalitic gneiss 467558 addressed above.

Table 3. Zircon U-Pb ion probe data, orthogneiss and granodiorite, Maniitsoq and adjacent islands

Spot #	Morphology	U ppm	Th ppm	Pb ppm	Th/U measured	f <sup>206</sup> %	<sup>207</sup> Pb/ <sup>206</sup> Pb	σ %	<sup>207</sup> Pb/ <sup>235</sup> U	σ %	<sup>206</sup> Pb/ <sup>238</sup> U	σ %	Disc. % (conv.)	Ages (Ma)					
														<sup>207</sup> Pb/ <sup>206</sup> Pb	σ	<sup>207</sup> Pb/ <sup>235</sup> U	σ	<sup>206</sup> Pb/ <sup>238</sup> U	σ
<b>Sample 467558, orthogneiss, island east of Maniitsoq (68°45.736'N, 52°50.254'W)</b>																			
1	c el pr osc	166	98	111	0.59	0.17	0.1970	0.35	13.263	1.09	0.4884	1.03	-10.3	2801	6	2699	10	2564	22
12	c el pr osc	280	100	193	0.36	0.02	0.1984	0.25	14.639	1.06	0.5351	1.03	-2.2	2813	4	2792	10	2763	23
11	fra e el pr osc	321	164	209	0.51	0.22	0.1915	0.26	12.934	1.06	0.4898	1.03	-8.2	2755	4	2675	10	2570	22
16	e el pr osc	189	106	122	0.56	0.49	0.1941	0.38	12.861	1.10	0.4805	1.03	-10.8	2778	6	2670	10	2529	22
28	c el pr osc	245	142	155	0.58	1.16	0.1928	0.31	12.405	1.07	0.4667	1.03	-12.9	2766	5	2636	10	2469	21
34	c el pr osc	233	99	156	0.43	0.22	0.1952	0.33	13.751	1.08	0.5109	1.03	-5.5	2786	5	2733	10	2661	22
38	c el pr osc	212	100	144	0.47	0.23	0.1953	0.29	13.826	1.07	0.5135	1.03	-5.0	2787	5	2738	10	2672	23
50	c el pr osc	270	125	154	0.46	1.02	0.1882	0.31	11.070	1.12	0.4267	1.07	-18.9	2726	5	2529	10	2291	21
60	c el pr osc	204	145	143	0.71	0.09	0.1958	0.29	13.590	1.09	0.5034	1.05	-7.1	2791	5	2722	10	2628	23
64	c el pr osc	145	72	103	0.50	0.07	0.1976	0.29	14.441	1.07	0.5302	1.03	-2.8	2806	5	2779	10	2742	23
66	c el pr osc	230	125	140	0.54	0.98	0.1918	0.28	12.065	1.07	0.4562	1.03	-14.5	2758	5	2609	10	2423	21
71	c pr osc	312	124	190	0.40	0.68	0.1890	0.44	12.110	1.33	0.4646	1.26	-12.0	2734	7	2613	13	2460	26
79	e pr osc	230	103	120	0.45	0.5	0.1923	0.39	10.432	1.17	0.3935	1.10	-26.4	2762	6	2474	11	2139	20
75	c pr osc	172	65	103	0.38	0.21	0.1938	0.32	12.323	1.08	0.4611	1.03	-14.3	2775	5	2629	10	2445	21
<b>Sample 467565, granodiorite, island south-west of Maniitsoq (68°45.047'N, 52°59.460'W)</b>																			
1	c el pr osc	633	376	434	0.59	0.36	0.1902	0.22	13.025	1.57	0.4966	1.55	-6.4	2744	4	2681	15	2599	33
2	c el pr osc	902	299	599	0.33	0.04	0.1929	0.12	13.714	1.56	0.5155	1.55	-3.8	2767	2	2730	15	2680	34
3	c el pr osc	494	340	312	0.69	0.14	0.1862	0.14	12.12	1.62	0.4722	1.61	-9.6	2709	2	2614	15	2493	33
4	c el pr osc	575	410	387	0.71	0.42	0.1921	0.16	13.125	1.56	0.4955	1.55	-7.3	2760	3	2689	15	2595	33
5	e el pr osc	913	792	656	0.87	0.12	0.1827	0.61	12.672	1.77	0.5030	1.66	-2.3	2678	10	2656	17	2627	36
6	e el pr osc	535	256	357	0.48	0.11	0.1939	0.22	13.629	1.67	0.5097	1.66	-5.3	2776	4	2724	16	2655	36
7	c el pr osc	509	160	356	0.31	0.20	0.1934	0.19	14.373	1.64	0.5390	1.62	0.4	2771	3	2775	16	2779	37
8	c el pr osc	737	318	514	0.43	0.04	0.1914	0.24	13.995	1.57	0.5305	1.55	-0.5	2754	4	2749	15	2743	35
9	c el pr osc	1048	768	822	0.73	0.02	0.1944	0.12	14.990	1.56	0.5594	1.55	3.8	2779	2	2815	15	2864	36
10	e el pr osc	2750	1074	1732	0.39	0.02	0.1843	0.17	12.359	1.57	0.4864	1.57	-6.1	2692	3	2632	15	2555	33
11	c el pr osc	624	280	347	0.45	0.13	0.1937	0.32	11.109	1.59	0.4160	1.55	-22.6	2774	5	2532	15	2242	29
12	e el pr osc	412	246	307	0.60	0.20	0.1937	0.21	14.462	1.58	0.5416	1.56	0.7	2773	3	2781	15	2790	35
13	e el pr osc	960	321	625	0.33	0.11	0.1873	0.20	13.056	1.57	0.5057	1.55	-3.6	2718	3	2684	15	2638	34
14	c el pr osc	303	161	214	0.53	0.10	0.1936	0.16	13.900	1.58	0.5207	1.57	-3.1	2773	3	2743	15	2702	35
15	e el pr osc	643	619	508	0.96	0.08	0.1936	0.12	14.308	1.56	0.5361	1.55	-0.3	2773	2	2770	15	2767	35
16	e el pr osc	1378	526	782	0.38	1.08	0.1901	0.13	10.673	1.56	0.4073	1.56	-23.2	2743	2	2495	15	2202	29
17	fra e el pr osc	804	308	439	0.38	0.47	0.193	0.17	10.821	1.61	0.4067	1.60	-24.2	2768	3	2508	15	2200	30
18	e el pr osc	830	292	573	0.35	0.02	0.193	0.10	14.173	1.56	0.5327	1.55	-0.7	2768	2	2761	15	2753	35
<b>Sample 467575, granodiorite, south coast of Maniitsoq (68°45.450'N, 52°53.230'W)</b>																			
1	fra e pr osc	1044	438	511	0.42	0.12	0.1760	0.20	9.095	1.58	0.3748	1.57	-25.1	2615	3	2348	15	2052	28
2	e pr osc	914	240	566	0.26	0.93	0.1660	0.25	11.053	1.60	0.4830	1.58	1.1	2517	4	2528	15	2540	33
2b		1188	339	825	0.29	0.92	0.1679	0.20	12.449	1.64	0.5378	1.63	11.6	2537	3	2639	16	2774	37
3b	e pr osc	1665	636	693	0.38	0.25	0.1565	0.29	7.068	1.61	0.3275	1.59	-28.0	2418	5	2120	14	1826	25
4	c eq pr osc	683	258	316	0.38	2.71	0.1667	0.35	7.941	1.70	0.3454	1.66	-28.0	2525	6	2224	15	1913	28
4b		819	424	306	0.52	4.14	0.1625	0.56	6.063	1.74	0.2706	1.65	-42.4	2482	9	1985	15	1544	23
5	c el pr osc	1255	617	559	0.49	1.53	0.1636	1.80	7.295	2.70	0.3233	2.01	-31.5	2494	30	2148	24	1806	32
5b		1429	548	626	0.38	1.46	0.1645	0.33	7.481	1.74	0.3299	1.71	-30.4	2502	6	2171	16	1838	27
6	fra e pr osc	315	186	150	0.59	0.99	0.1844	0.22	8.976	1.64	0.3531	1.62	-31.9	2692	4	2336	15	1950	27
7	fra c pr osc	954	422	539	0.44	0.14	0.1859	0.19	11.201	1.63	0.4371	1.61	-16.2	2706	3	2540	15	2337	32
8	c pr osc	212	170	139	0.80	0.43	0.1893	0.23	12.030	1.71	0.4609	1.70	-12.8	2736	4	2607	16	2444	35
9	c el pr osc	629	245	365	0.39	0.44	0.1858	0.22	11.362	1.72	0.4435	1.71	-14.9	2705	4	2553	16	2366	34
10	e el pr osc	77	54	57	0.70	0.15	0.2005	0.33	14.804	1.62	0.5354	1.59	-2.9	2831	5	2803	16	2764	36
11	c el pr osc	393	1343	404	3.42	0.55	0.193	0.18	12.870	1.68	0.4836	1.67	-9.8	2768	3	2670	16	2543	35
12	c el pr osc	761	436	376	0.57	0.70	0.1704	0.34	8.673	1.61	0.3691	1.57	-24.4	2562	6	2304	15	2025	27
13	fra c el pr osc	398	263	218	0.66	0.29	0.1626	0.31	8.894	1.72	0.3968	1.70	-15.6	2483	5	2327	16	2154	31
14	fra c pr osc	971	219	404	0.23	0.79	0.1409	0.32	6.484	1.63	0.3337	1.60	-19.6	2239	5	2044	14	1856	26
15	c el pr osc	326	61	164	0.19	0.43	0.1762	0.25	9.906	1.59	0.4076	1.57	-18.6	2618	4	2426	15	2204	29
16	c pr osc	195	129	144	0.66	0.43	0.1896	0.23	13.889	1.59	0.5312	1.57	0.3	2739	4	2742	15	2747	35
17	c el pr osc	798	159	365	0.20	0.56	0.1673	0.27	8.413	1.61	0.3647	1.58	-24.1	2531	5	2277	15	2004	27
18	e el pr osc	935	298	468	0.32	1.07	0.1619	0.22	8.712	1.61	0.3903	1.60	-16.6	2475	4	2308	15	2124	29
19	fra e pr osc	947	302	419	0.32	1.29	0.1499	0.56	7.024	1.67	0.3397	1.57	-22.6	2345	10	2114	15	1885	26
20	e el pr osc	844	297	442	0.35	0.05	0.1627	0.27	9.211	1.61	0.4105	1.59	-12.7	2484	4	2359	15	2217	30
21	c el pr osc	689	568	385	0.82	0.38	0.1828	0.28	9.916	1.88	0.3934	1.86	-23.6	2678	5	2427	18	2139	34

Errors on ratios and ages are quoted at 1σ level; f<sup>206</sup> %: The fraction of common <sup>206</sup>Pb, estimated from the measured <sup>204</sup>Pb; Disc. % (conv.): Degree of discordance of the zircon analysis (at the centre of the error ellipse). Grain morphology: c: core; e: edge (i.e. edge of grain, not a distinct rim); el: elongate; fra: fragment; pr: prismatic (i.e. euhedral grain shape); osc: oscillatory zoned.

## The national map sheet coverage

---

**Greenland**  
**1:100 000**

